Study on cellular response to compressive stress in mouse myoblasts: Involvement of dephosphorylation of the myosin regulatory light chain via RhoA phosphorylation

（マウス筋芽細胞における圧縮刺激に対する細胞応答に関する研究：RhoA のリン酸化によるミオシン調節軽鎖の脱リン酸化の関与）

Kenji Takemoto

2015

Doctoral Dissertation

Transdisciplinary Life Science Course

Graduate School of Life Science

Hokkaido University

Contents

Abbreviations

1P-MRLC: phosphorylated myosin regulatory light chain (Ser19)

2P-MRLC: phosphorylated myosin regulatory light chain (Thr18/Ser19)

ADP: adenosine diphosphate

ATP: adenosine triphosphate

cAMP: cyclic adenosine monophosphate

ECM: extracellular matrix

F-actin: filamentous actin

GAP: GTPase-activating protein

GDP: guanosine diphosphate

GEF: guanine nucleotide exchange factors

GTP: guanosine triphosphate

MELC: myosin essential light chain

MLCP: myosin light chain phosphatase

MRLC: myosin regulatory light chain

MYPT1: myosin phosphatase targeting subunit 1

PKA: protein kinase A

PP1cδ: protein phosphatase 1cδ

ROCK: Rho-associated, coiled-coil containing protein kinase

SFTI: stress fiber thickness index

SEM: standard error of the mean

TAZ: transcriptional coactivator with PDZ-binding motif

YAP: Yes-associated protein

Chapter 1

General Introduction

1.1 Background

1.1.1 Mechanical stress

Organisms are always subjected to external stresses. The stresses have various kinds such as physiological, biochemical, and mechanical one. In this study, we focused on effects of mechanical stress on tissues and cells that constitute mammals. Mechanical stress is a stimulation that applies external force to cells (gravity, shear stress, pressure, deformation, etc.). In order to maintain cell homeostasis, it is necessary for cells to respond to mechanical stress. For example, vascular smooth muscle cells dilate and constrict in response to variations in blood pressure. High blood pressure causes an increase in blood flow and shear stress on vascular endothelial cells resulting in vascular damage. On the other hand, low blood pressure reduces blood circulation making it more difficult to provide nutrients and oxygen throughout the body. Therefore, in order to maintain constant blood flow, smooth muscle cells contract or dilate in response to high or low blood pressure (Kuo *et al*., 1993; Osol *et al*., 2002). Dysfunctional response to blood pressure induces several vascular diseases, such as hypertension (Izzard *et al*., 2003), chronic heart failure (Gschwend *et al*.,2003) and vasospastic angina (Masumoto *et al*., 2002). Thus,

elucidating the cellular response to different mechanical stress in the human body is important for understanding various physiological events, including disease development.

1.1.2 Mechanotransduction and mechanosensor

As mentioned above, cells can sense and respond to mechanical stress. The mechanism by which cells convert mechanical signals into biochemical responses is called mechanotransduction, and proteins that trigger the mechanotransduction is called mechanosensors. Heretofore, multiple mechanosensors have been found. For example, stretch-activated ion channels (SA channels) open and allow the influx of calcium ions in response to membrane tension (Coste *et al*., 2010). The glycocalyx, a layer of proteoglycans and glycoproteins on the endothelial cell surface, can induce mechanotransduction in response to fluid shear stress (Weinbaum *et al*., 2003). External forces can induce conformational changes in cytoskeletal components such as actin filaments (Hara *et al*., 2001) and cross-linker filamins (Ehrlicher *et al*., 2011), thereby changing binding affinities of effectors to these proteins. In this manner, new mechanosensors have been found one after another. However, the mechanism how some mechanosensors sense mechanical stress were unknown.

1.1.3 Cellular response to mechanical stress via deformation of extracellular matrix

Mechanical stress that arises due to deformation of extracellular matrix (ECM) is divided broadly into two categories: stretch and compression. The cellular response to stretching cells has been widely studied. For example, stretched cardiac fibroblasts showed increases in collagen type I, III, and fibronectin expression by TGF-β-dependent pathway (Lee *et al*., 1999). Mouse myoblasts activates cell proliferation (Kook *et al*., 2008) and differentiates into myotube (Zhan *et al*., 2007) via MAPK activation in response to stretching stress. Our group has found that cellular elasticity measured by using atomic force microscopy were increased 10 minutes after cells were stretched uniaxially (Mizutani *et al*., 2004). Additionally, the response was associated with phosphorylation of myosin regulatory light chain through RhoA/ROCK pathway (Mizutani *et al*., 2009), which referred to the chapter 2 and 6 for more details. On the other hand, cellular responses to compressive loading are not well understood. It is also unclear which proteins can sense differences between stretching and compressing cells.

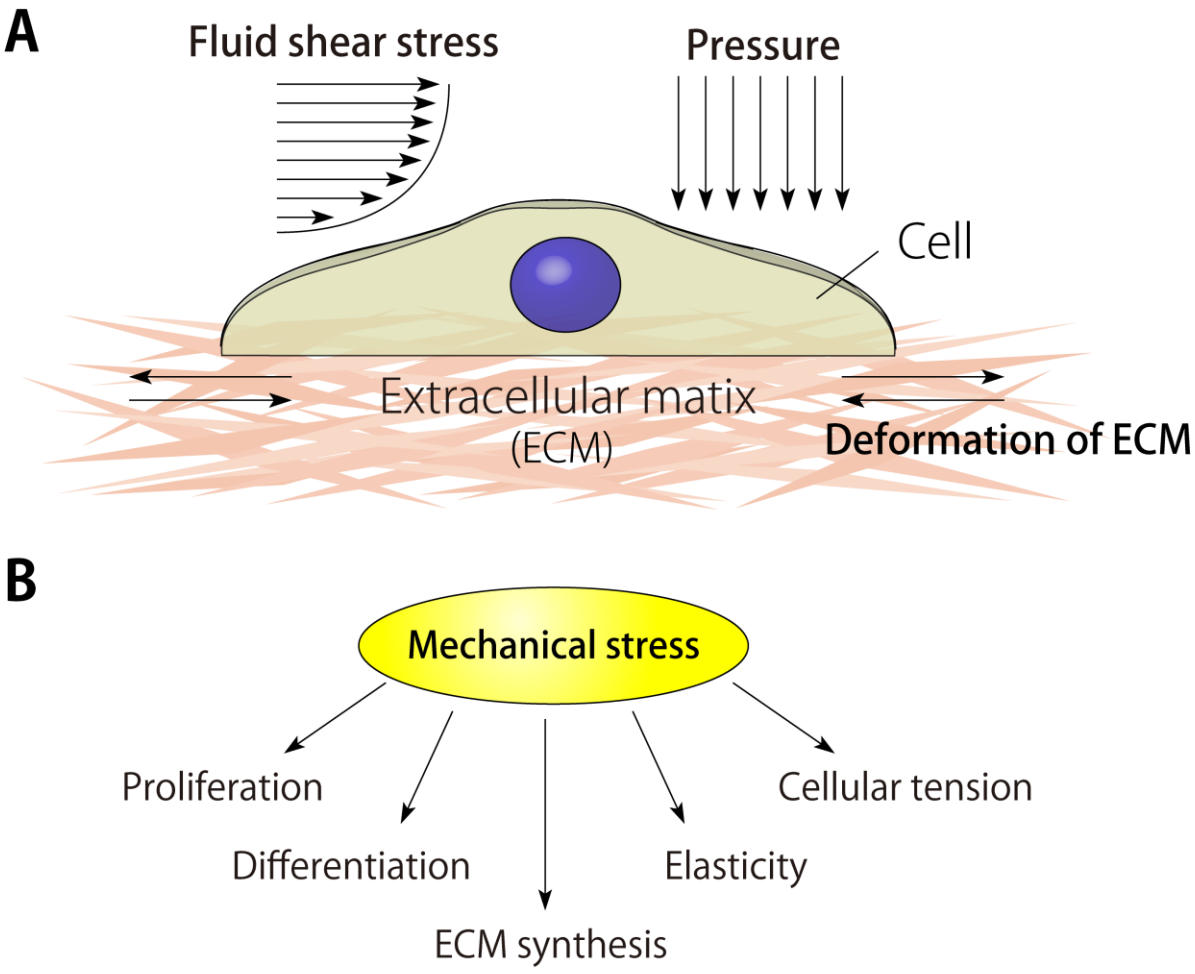

Figure 1-1. Cellular mechanotransduction

(A) The shematic image of various mechanical stresses applied to cells

(B) Effects of mechanical stress on cellular physiological function

1.2 Purpose

Cellular responses to compressive stress are less investigated than the responses to stretching stress. The mechanism how cells sense the difference between stretched and compressed stresses is still unclear.

This study tried to investigate the mechanism how cells sense the difference between stretched and compressed stresses. Specifically, we checked whether phosphorylation levels of MRLC were changed by compressive loading.

1.3 Materials and methods

1.3.1 Cell culture

Murine C2C12 skeletal myoblast cells were obtained from the RIKEN Cell Bank (Tsukuba, Japan). Cells were cultured in Dulbecco's modified Eagle's medium (DMEM; Sigma-Aldrich, MO, USA) supplemented with 10% fetal bovine serum (BIST-TEC; Equitech Bio Inc., TX, USA) and 1% antibiotic solution (Sigma-Aldrich) at 37 °C in a humidified atmosphere of 5% CO_2.

1.3.2 Reagents

Protein phosphatase 1 and 2A inhibitor (Calyculin A), protein kinase A inhibitor (H-89), and adenylyl cyclase inhibitor (SQ22,536) were purchased from Sigma-Aldrich. The following primary antibodies were used for western blotting: myosin light chain 2 antibody (#3672; Cell Signaling Technology, MA, USA), phospho-myosin light chain 2 (Ser19) antibody (#3671; Cell Signaling Technology), phospho-myosin light chain 2 (Thr18/Ser19) antibody (#3674; Cell Signaling Technology), myosin light chain 2 antibody (#3672; Cell Signaling Technology), GAPDH antibody (#AM4300; Ambion, TX, USA), MYPT1 antibody (#2634; Cell Signaling

Technology), phospho-MYPT1 (Thr696) antibody (#5163; Cell Signaling Technology), phospho-MYPT1 (Thr853) antibody (#4563; Cell Signaling Technology), RhoA antibody (#ARH03; Cytoskeleton, CO, USA), and phospho-RhoA (Ser188) antibody (#AB41435; Abcam, Cambridge, UK). MRLC stained by phospho-myosin light chain 2 (Ser19) antibody is denoted as 1P-MRLC, and MRLC stained by phospho-myosin light chain 2 (Thr18/Ser19) antibody is denoted as 2P-MRLC.

1.3.3 Application of mechanical strain

Cells were stretched or compressed isotropically using previously described methods (Kawamoto *et al*., 2008). The silicone chamber and steel ring were prepared, as shown Figure 1-1. The chamber is made of a transparent silicone rubber (SH9555; Toray Dow Corning Silicone, Tokyo, Japan). For cell compression, the silicone chamber was pre-stretched by inserting the steel ring into the ditch of silicone. Myoblast cells were removed from the culture dishes using trypsin-EDTA, transferred to the chamber, and cultured on pre-stretched silicone coated with 50 μg/mL fibronectin. When the ring was pulled out of the ditch, the cells were compressed via the compression of the silicone chamber (Fig. 1B). We observed that

cell area was decreased 14% immediately after cell compression (Fig. S2C). In order to perform cell stretching, cells were cultured on the silicone chamber which was not pre-stretched, and then stretched by inserting the steel ring into the ditch of silicone (Fig. 1C). The medium was replaced with DMEM containing 1% FBS and 1% antibiotic solution for 3 hours before applying mechanical strain. The cells were treated with the following inhibitors for 90 minutes before mechanical loading: 2 nM calyculin A (Sigma-Aldrich), 30 μM H-89 (Sigma-Aldrich), and 100 μM SQ22,536 (Sigma-Aldrich).

1.3.4 Western blotting

Cells were fixed in ice-cold trichloroacetic acid for 3 minutes and washed 3 times with PBS. Cell lysates were prepared in Laemmli sample buffer (0.25 M Tris-HCl, 5% dithiothreitol, 2.3% sodium dodecyl sulfate, 10% glycerol, 0.01% bromophenol blue, pH 8.8). The proteins were then separated by SDS-PAGE using 7.5% polyacrylamide gels (for MYPT1) and 12.5% (for other proteins). After blocking (5% skimmed milk in TBS-Tween 20 solution, 10 mM Tris-HCl containing 150 mM NaCl and 0.05% Tween 20, pH 7.5), the blots were incubated at 4 °C overnight with the appropriate primary antibody. After incubation with a secondary antibody (HRP-

conjugated anti-mouse or anti-rabbit IgG), the blots were developed using Can Get Signal Immunoreaction Enhancer Solution (Toyobo, Osaka, Japan). Protein levels of GAPDH were used as an internal standard. Western blots were quantified by Image J software (National Institutes of Health, Bethesda, MA).

1.3.5 Observation of actin filaments

To observe the dynamics of F-actin in cells under compressive loading, we performed live cell imaging. Semi-confluent C2C12 cells on a culture dish were transfected with a previously constructed plasmid encoding azami green-tagged β-actin (Tamura *et al*., 2011) and cultured for 1 day. The cells were removed from the culture plate using trypsin-EDTA, transferred onto the silicone chamber, and observed with a Nikon C1 confocal imaging system (Nikon Instech., Tokyo, Japan).

To assess the thickness of F-actin in cells under compressive strain, we performed immunofluorescent staining. Cells were fixed with 4% paraformaldehyde in PBS for 10 minutes, permeabilized with 0.5% Triton X-100 in PBS for 10 minutes. The samples were then blocked with 0.5% BSA in PBS for 1 hour at room temperature, and incubated with MFP 488-phalloidin for 1 hour at room temperature. We observed the samples after treatment with a fade-resistant solution

(2.5% DABCO, 90% glycerol, 6% PBS; pH 8.0). The resulting images were captured with a Nikon C1 confocal imaging system using the ×60 objective (Nikon Instech.).

1.3.6 Quantitative analysis of actin filament thickness

The thickness of F-actin was quantitatively analyzed with a stress fiber thickness index (SFTI) (Yoshigi *et al*., 2005). In brief, immunofluorescent images of actin filaments were subjected to a minimum filter, which replaced each pixel in the image with the smallest pixel value in that pixel's neighborhood. Fluorescence intensities on F-actin were gradually decreased by repeating minimum filtering. Actin filament intensity against the number of minimum filtering was fitted using the following equation:

$$I = A + B \cdot \exp\left(-\frac{N}{\tau}\right)$$

where I is fluorescence intensity on a F-actin image, N is the number of the minimum filtering, τ is the decay constant, and A and B are constants. The fluorescence intensity of thicker fibers decayed slower with filtering; thus, the decay constant was associated with actin filament thickness. The decay constant τ was used as a SFTI. Images of phalloidin-stained actin filaments in 60 individual cells were randomly selected from 3 independent experiments and analyzed.

1.3.7 RNA interference (RNAi)

RNAi was used to knockdown the expression of the MYPT1 gene. The target sequence of the siRNA used in this study was 5′-CUGUGGAUAUCUCGAUAUUGC-3′ (sense sequence). As a negative control, the following non-target sequence of the siRNA was randomly selected and used: 5′-ACUACAUGUCACAUCACGGUU-3′ (sense sequence). Cells were transfected with siRNA duplexes using Lipofectamine™ RNAiMAX (Invitrogen, CA, USA) and were used for the designated assay after incubation for 2 days. The silencing efficiency was confirmed by western blotting.

1.3.8 RhoA activation assay

The Rho activity assay was performed and quantified using the RhoA Activation Assay Biochem Kit (Cytoskeleton) based on the Rhotekin pull-down assay. In brief, cells were washed with PBS then extracted using cell lysis buffer (50 mM Tris, pH 7.5, 10 mM $MgCl_2$, 0.5 M NaCl, 2% Igepal). Samples were centrifuged for 5 minutes at 10,000 × *g* and then the supernatant was incubated with Rhotekin-RBD beads for 1.5 hours at 4 °C. After washing the beads with buffer (25 mM Tris, pH 7.5, 30 mM $MgCl_2$, 40 mM NaCl), proteins were removed from the beads with Laemmli buffer,

then subjected to western blotting.

1.3.9 Statistical analysis

Statistical analysis of the western blot data was performed using the Student's *t*-test. Data is presented as mean ± standard error of the mean (SEM), and consists of 3 independent experiments.

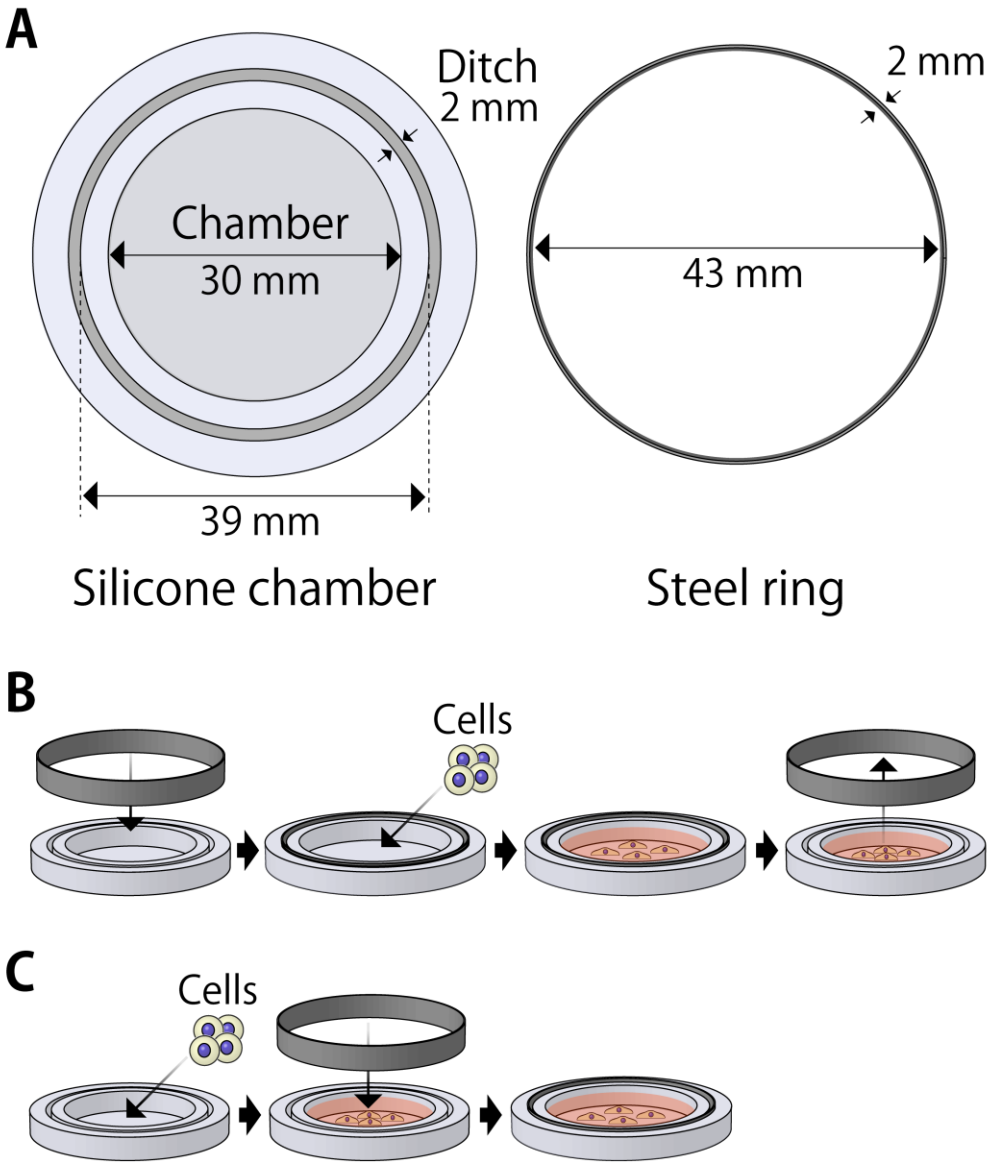

Figure 1-2. The methods for application of mechanical strain

(A) An overview of the isotropic deformation device consisting of a silicone chamber and a steel ring. When the steel ring was inserted into the silicone ditch, the silicone chamber was 39 mm in diameter.

(B) Method for compressing cells. A silicone chamber is pre-extended by inserting a steel ring into a ditch. Cells are seeded on the pre-extended silicone chamber, and compressed by pulling out a steel ring from a ditch.

(C) Method for stretching cells. Cells are cultured on a silicone chamber without inserting a steel ring. By inserting a steel ring into a ditch, cells are stretched.

Chapter 2

MRLC dephosphorylation in response to cell compression

2.1 Introduction

2.1.1 Cellular contractile force

Cells can generate a contractile force by themselves and perform cellular migration, cytokinesis and morphological maintenance by using the tension (Paluch and Heisenberg, 2009; Rappaport, 1967; Vicente-Manzanares *et al*., 2008). The complex composed of actin cytoskeleton and myosin II motor protein plays a role to exert the force in cells. Actin cytoskeleton exists as a globular monomer and forms a spiral filament by the polymerization of actin monomers (Oda *et al*., 2009). The actin filaments network is spread on the whole of cell surface. The fibers act as skeletal frames to form into various cell shapes and as rails to transport endoplasmic reticulum (Bathe *et al*., 2008; Krendel and Mooseker, 2005). Myosin II is comprised of two heavy chains, two regulatory light chains (MRLCs) and two essential light chains (MELCs) (Figure 2-1). Myosin heavy chain is divided into head, neck and tail domain. The head domain has actin binding and ATPase activity, neck domain interacts with MRLC and MELC, and the tail domains in myosins are bound with each other, which resulted in formation of bipolar myosin filaments (Holmes. 2008). MELC stabilizes conformation of myosin heavy chain, and deficiency of MELC

suspended myosin function (Hernandez *et al*., 2007). MRLC regulates ATPase activity of myosin (Somlyo and Somlyo. 2003).

The mechanism how actin and myosin generate force is briefly described below (Yanagida *et al*., 1985). Myosin repeats the cycle of binding to actin and releasing by the use of chemical energy generated by ATP hydrolysis, which resulted in products of forces (Figure 2-2). First, ADP-bound myosin can attach to an actin filament. When the myosin release ADP and phosphate, the neck domain in myosin changes its conformation. Thereby, the myosin applies force and displaces an actin filament. New ATP binds to the free myosin, then the myosin liberate F-actin. Myosin hydrolyses ATP to return to the first step of the cycle. The higher ATPase activity myosins have, the stronger force cells generate.

2.1.2 Regulation of cellular contractile force by MRLC phosphorylation

As mentioned above, myosin ATPase activity is associated with strength of cellular force. The ATPase activity is regulated by phosphorylation levels of MRLC. Phosphorylation sites of MRLC are two residues: Thr18 and Ser19 (Hirata *et al*., 2009; Somlyo and Somlyo. 2003). Ser19 phosphorylation in MRLC causes not only up-regulation of myosin ATPase activity but also conformation change of an entire

myosin heavy chain (Somlyo and Somlyo. 2003). In unphosphorylated state of MRLC, myosin forms a compact conformation by the head–head and head–tail interactions (Figure 2-1) (Wendt *et al*., 2001). This condition blocks myosin filament assembly and interaction with F-actin. Phosphorylation of MRLC (Ser19) prevents the interactions between head–head and head–tail domains and converts the folded into the extended comformation. The Thr18 site on MRLC is phosphorylated subsequently to Ser19 phosphorylation (Hirata *et al*., 2009). Di-phosphorylated MRLC (Thr18 and Ser19) more effectively activates myosin ATPase activity than mono-phosphorylated MRLC (Ser19) (Umemoto *et al*., 1989).

2.1.3 Effects of mechanical stress on phosphorylation levels of MRLC

It is reported that phosphorylation levels of MRLC change in response to various mechanical stress. For example, Laminar shear stress induced phosphorylation of MRLC and cause higher traction forces in endothelial cells (Nakai *et al*., 1997). Mesenchymal stem cells cultured on stiffer extracellular matrix (ECM) had more phosphorylated MRLC and resulted in osteogenic differentiation (Shih *et al*., 2011). Our group reported that when mouse fibroblast cells (NIH-3T3) was stretched by deformation of the elastic substrate where cells was cultured, MRLC was phosphorylated within 15 minutes (Mizutani *et al*., 2009). However, it was unclear

whether compressive loading affects phosphorylation levels of MRLC.

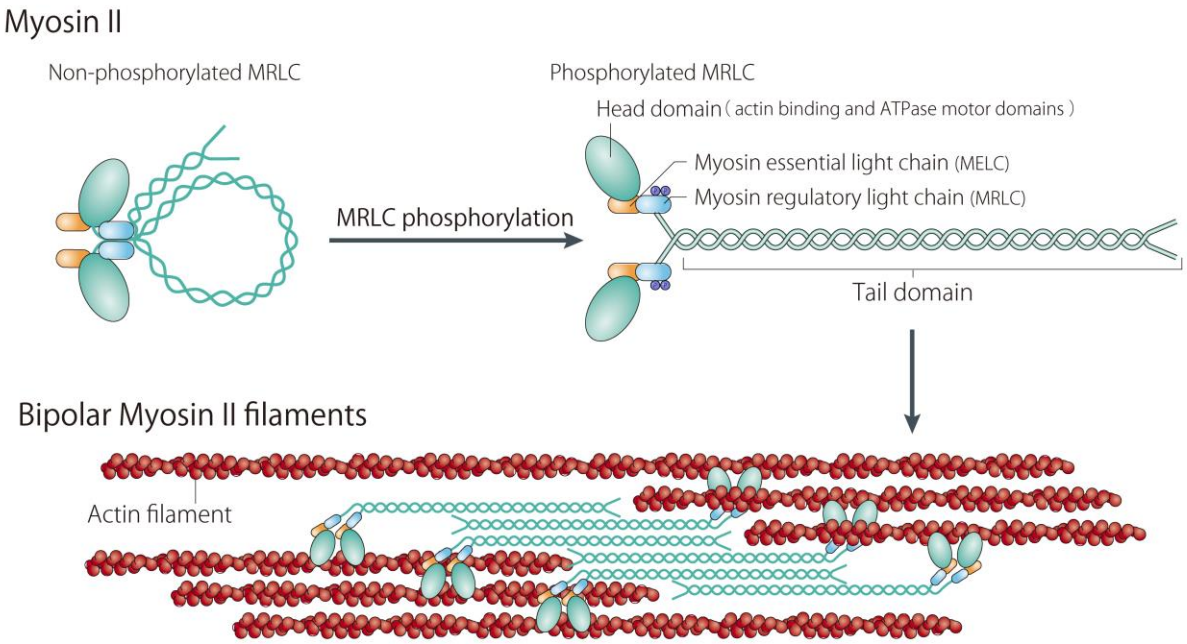

Figure 2-1. Structure of myosin II (Vicente-Manzanares *et al.*, 2009)

The myosin II forms a dimer through interactions between the α-helical coiled-coil tail domains. The head domain contains the actin-binding regions and the enzymatic ATPase motor domains. The essential light chains (MELCs) and the regulatory light chains (MRLCs) bind to the heavy chains at the neck domains. In the absence of MRLC phosphorylation, myosin II forms a compact shape (upper left) that is unable to associate with actin filaments. On MRLC phosphorylation, the compact structure becomes an extended form (upper right). The extended myoins assemble into bipolar filaments through interactions between their tail domains. These filaments bind to actin through their head domains. The ATPase activity of myosin II enables a conformational change that moves actin filaments (bottom).

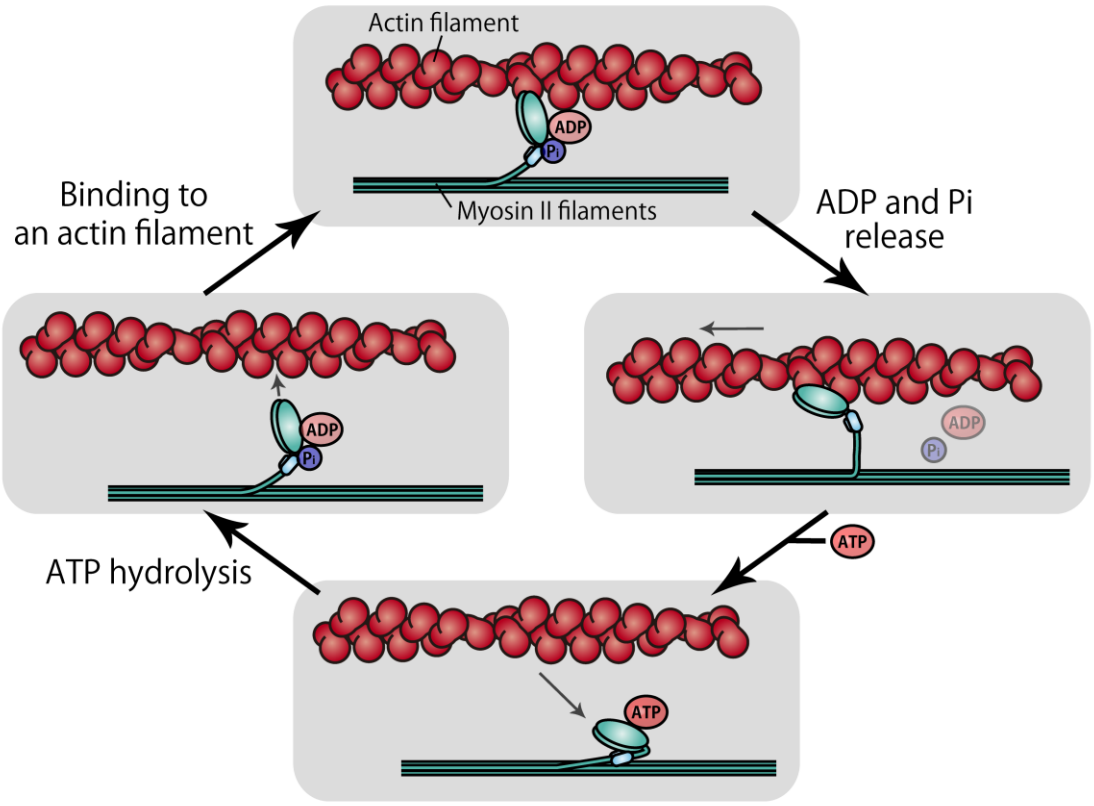

Figure 2-2. The mechanism of myosin power stroke

First, the ADP-bound myosin head domains attach to the actin (upper image). The ADP and phosphate is released, causing conformational change in myosin (right image). This triggers a power stroke. The power stroke is the force-generating step that causes the actin to slide along the myosin. When the ATP is bound, the myosin head domains reduce its binding affinity for actin and release the actin filament (bottom image). ATP is then hydrolysed, providing the energy to cock the myosin filaments (left image). This step allows the myosin head domains to bind to the actin filament, returning to the first step.

2.2 Results

We examined whether the phosphorylation levels of myosin regulatory light chain (MRLC) in C2C12 cells changed after 14% cell compression. In order to investigate time-dependent changes in MRLC phosphorylation, we analyzed mono-phosphorylated MRLC at Ser19 (1P-MRLC) and di-phosphorylated MRLC at Thr18 and Ser19 (2P-MRLC) by western blot at 0.5, 1, 3, and 5 minutes after compression (Figure 2-3A). The levels of phosphorylated MRLC 5 minutes after compressive loading decreased relative to the control without compressive stress. To determine whether MRLC underwent continued dephosphorylation for more than 5 minutes after compressive loading, we detected phosphorylated MRLC at 5, 15, and 30 minutes after cell compression (Figure 2-3B). Similar to Figure 2-3A, MRLC was dephosphorylated 5 minutes after cell compression. Fifteen minutes after compressive loading MRLC was more phosphorylated than at 5 minutes after cell compression. Furthermore, 15 minutes after cell compression the level of MRLC phosphorylation returned to the level reported before cell compression. Therefore, MRLC was significantly dephosphorylated in C2C12 cells 5 minutes after compression to 14%, but returned to the control levels by 15 minutes after compressive loading.

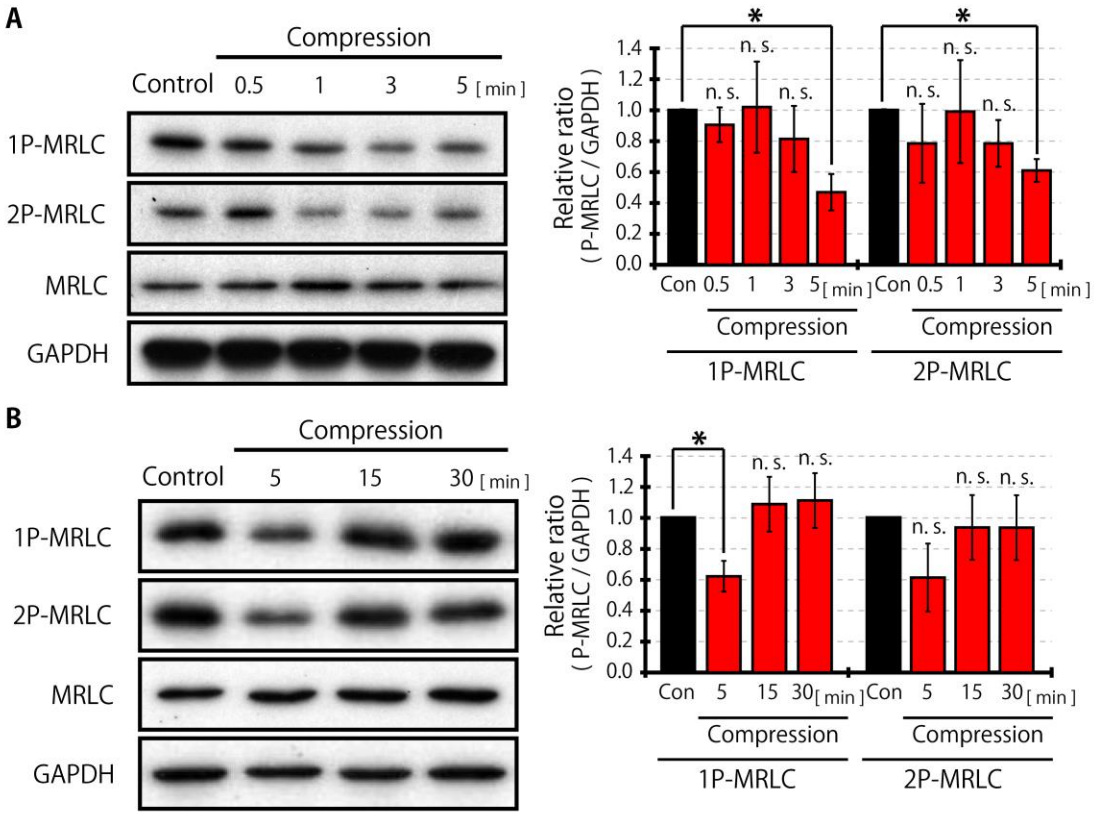

Figure 2-3. Phosphorylation of myosin regulatory light chain in response to compression

The phosphorylation levels of myosin regulatory light chain (MRLC) in C2C12 cells stimulated by 12% compression was detected by western blotting. Mono-phosphorylated MRLC (Ser19) is expressed as 1P-MRLC, and di-phosphorylated (Thr18/Ser19) is 2P-MRLC. Cells without compression were used as a control, and the compressed cells were analyzed at 0.5, 1, 3, and 5 minutes (A) and 5, 15, and 30 minutes (B) after compression. The levels of 1P-MRLC, 2P-MRLC, MRLC and GAPDH were quantified with Image J software. Quantification of western blots represents an average of 3 independent experiments, mean ± SEM. *, $p < 0.05$. n. s. stand for non significant difference between control and compression sample.

Chapter 3

14% compression did not affect actin filaments in C2C12 cells

3.1 Introduction

Next, we explored the mechanism of MRLC dephosphorylation in response to cell compression, we examined whether F-actins were disrupted by compressive loading.

Here we refer two reports. One report is that compressive loading induced F-actin disruption. Hayakawa *et al*. prepared human umbilical vein endothelial cells expressing GFP-tagged actin-severing protein (cofilin). When the cells were compressed (20%), GFP-cofilin were transferred to actin filaments within 1 minute. These fibers were disassembled within 30 minutes. Another report is that the treatment of the actin polymerization inhibitor induced dephosphorylation of MRLC. Mehta *et al*. reported that treatment of cytochalasin D significantly reduced both force development and phosphorylation levels of MRLC in canine tracheal smooth muscle.

We hypothesized that F-actin depolymerization by compressive stress induced MRLC dephosphorylation. However, it was unknown whether F-actin was disrupted after C2C12 cells were compressed (14%). Then, we observed F-actin dynamics by using live cell imaging and immunofluorescent staining technique 1 and 5 minutes after C2C12 cells were compressed.

14%

3.2 Results

We observed the behavior of actin filaments in cells expressing azami green-acitn (Figure 3-1). Live cell imaging showed that F-actin was not disrupted after cell compression. Even without significant disruption of actin filaments, the thickness of actin filaments might change in response to compressive loading. The thickness of actin filaments was quantitatively assessed using immunofluorescent techniques (Figure 3-2A). Actin filament thickness was estimated by the stress fiber thickness index (SFTI). SFTIs were not statistically different before or after compressive loading (Figure 3-2B). Thus, these results suggested that 14% compressive stress did not affect F-actin dynamics.

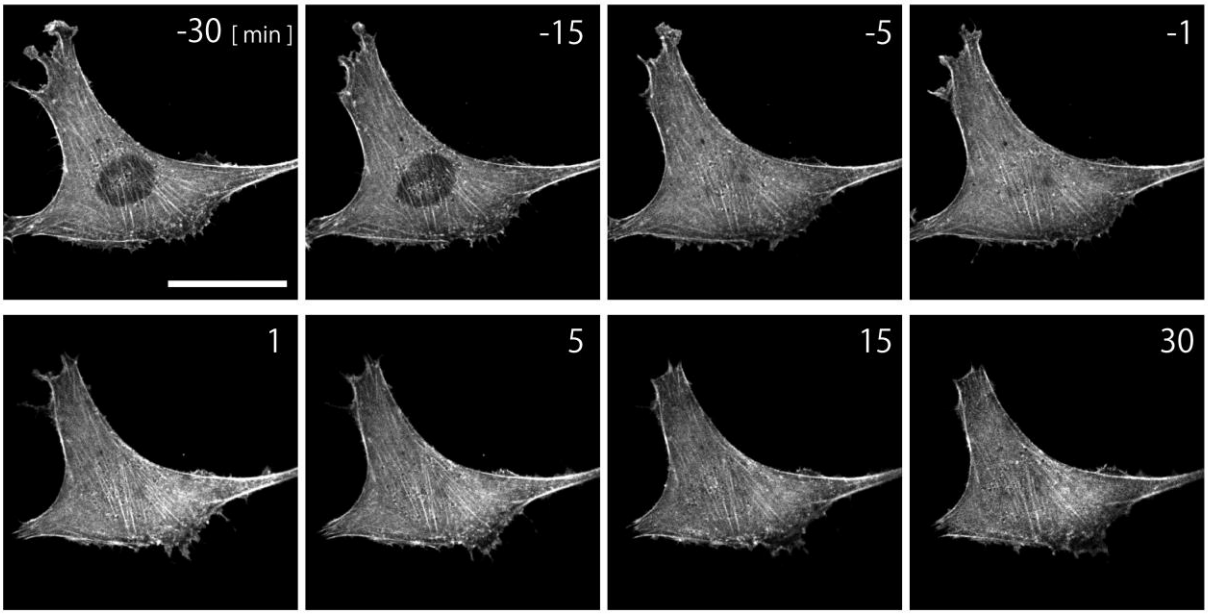

Figure 3-1. F-actin was not disrupted by compressive stress in living cells

Live imaging of cells expressing azami green-actin under compressive loading. Numbers at upper right in images are relative time (min) from the onset of compressive loading. Scale bar is 50 μm.

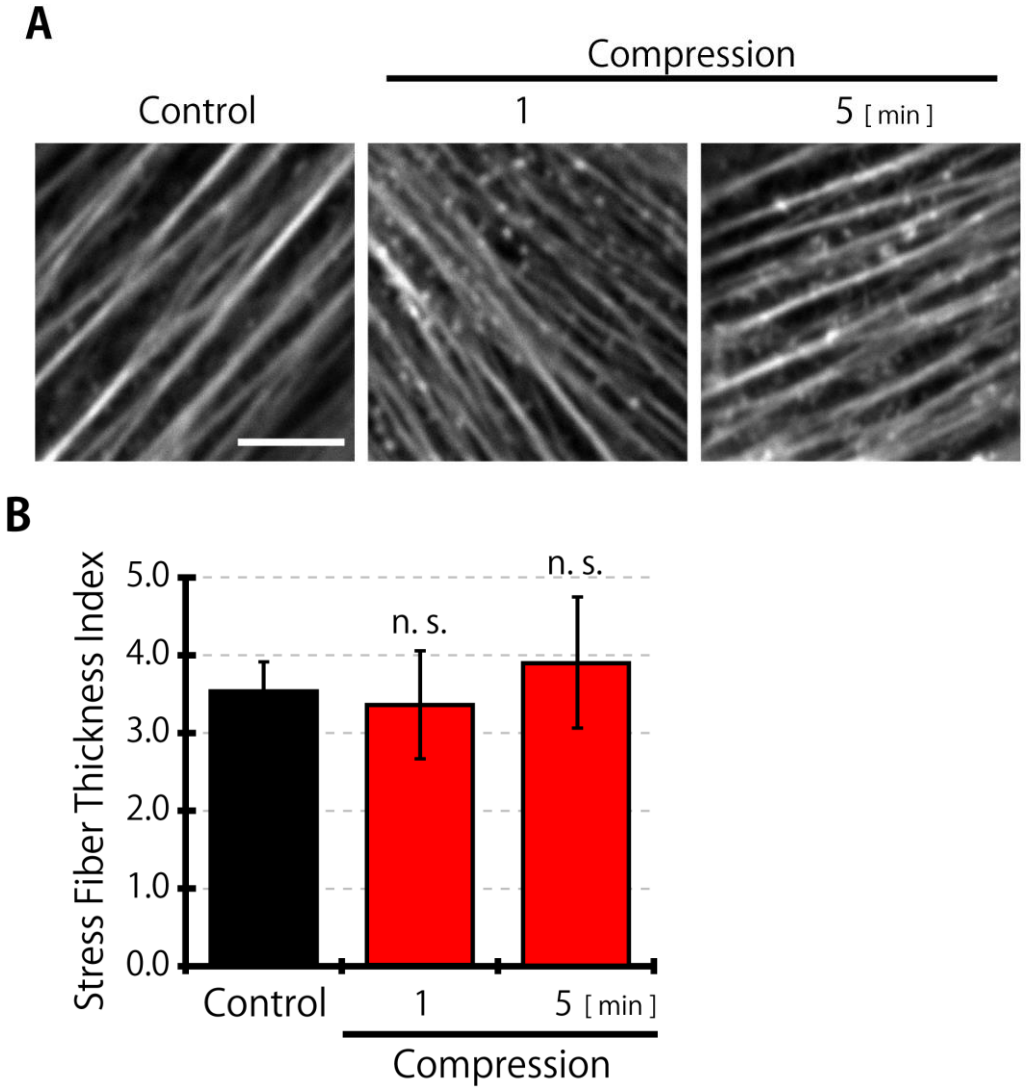

Figure 3-2. The observation of F-actin thickness before and after cell compression

(A) Immunofluorescent imaging of F-actin in cells before and after induction of compression. We observed F-actin stained with MFP 488-phalloidin in cells before and after compressive strain. Scale bar is 5 μm.

(B) Stress fiber thickness index in cells under compressive stress. By analyzing immunofluorescent images of F-actin, we assessed the thickness of F-actin in the form of stress fiber thickness index. The thicker actin filaments have a larger value of stress fiber thickness index. Image J software was used to estimate the thickness of F-actin. The stress fiber thickness index was calculated from 3 independent experiments including 60 individual cells. The results were presented as mean ± SEM. n. s. stand for non significant difference between control and compression sample.

Chapter 4

Compression induced MRLC dephosphorylation via activation of myosin light chain phosphatase

4.1 Introduction

4.1.1 Myosin light chain phosphatase (MLCP)

Compressive loading did not affect F-actin dynamics, so that thereafter we focused on phosphatase of MRLC.

Only one type of protein phosphatase (PP), called myosin light chain phosphatase (MLCP), dephosphorylates MRLC. MLCP is composed of three subunits: a catalytic subunit (protein phosphatase 1cδ, PP1cδ), a myosin binding regulatory subunit (myosin phosphatase target subunit 1, MYPT1), and a subunit of unknown function (p20) (Hartshorne, 1998). PP1cδ is one isoform of serine/threonine protein phosphatase 1 and involved in regulation of many cellular functions. MYPT1 acts as a platform for multiple interactions. N-terminal KVKF motif (residues 35 to 38) in MYPT1 interacts with PP1cδ (Ito *et al*., 2004). Binding site to phosphorylated MRLC in MYPT1 is controversial issue and may be at N-terminal ankyrin repeats or C-terminal region (Hartshorne, 1998). MYPT1 facilitates the specific activity of PP1cδ in the dephosphorylation of phospho-MRLC by tethering the catalytic subunit to MRLC. Therefore, MLCP activity is affected by external regulation of PP1cδ and MYPT1 (inactivation of PP1cδ by treatments with the inhibitor and knockdown of MYPT1 expression with RNAi technique).

4.1.2 Regulation of MLCP

MYPT1 is a not only platform for protein interactions but also regulator of MLCP activity. Thr694 and/or Thr852 at MYPT1 can be phosphorylated. Phospho-MYPT1 is also a target of PP1cδ, and lowers substrate specificity of PP1cδ to MRLC (Kiss *et al*., 2002; Takizawa *et al*., 2002; Hudson *et al*., 2012). Additionally, phosphorylation of MYPT1 (Thr852) interferes with the binding of MYPT1 to MRLC (Velasco *et al*., 2002). For these reasons, phosphorylation of MYPT1 inactivates MLCP. In contrast, blockage of MYPT1 phosphorylation induces MLCP activation. MYPT1 mutants (Thr694Ala and Thr852Ala) mimick the un-phosphorylated state, can enhance MLCP activity and decreases the levels of phosphorylated MRLC compared to wild type MYPT1 (Khromov *et al*., 2009). Therefore, MLCP activity is estimated by checking the phosphorylation levels of MYPT1.

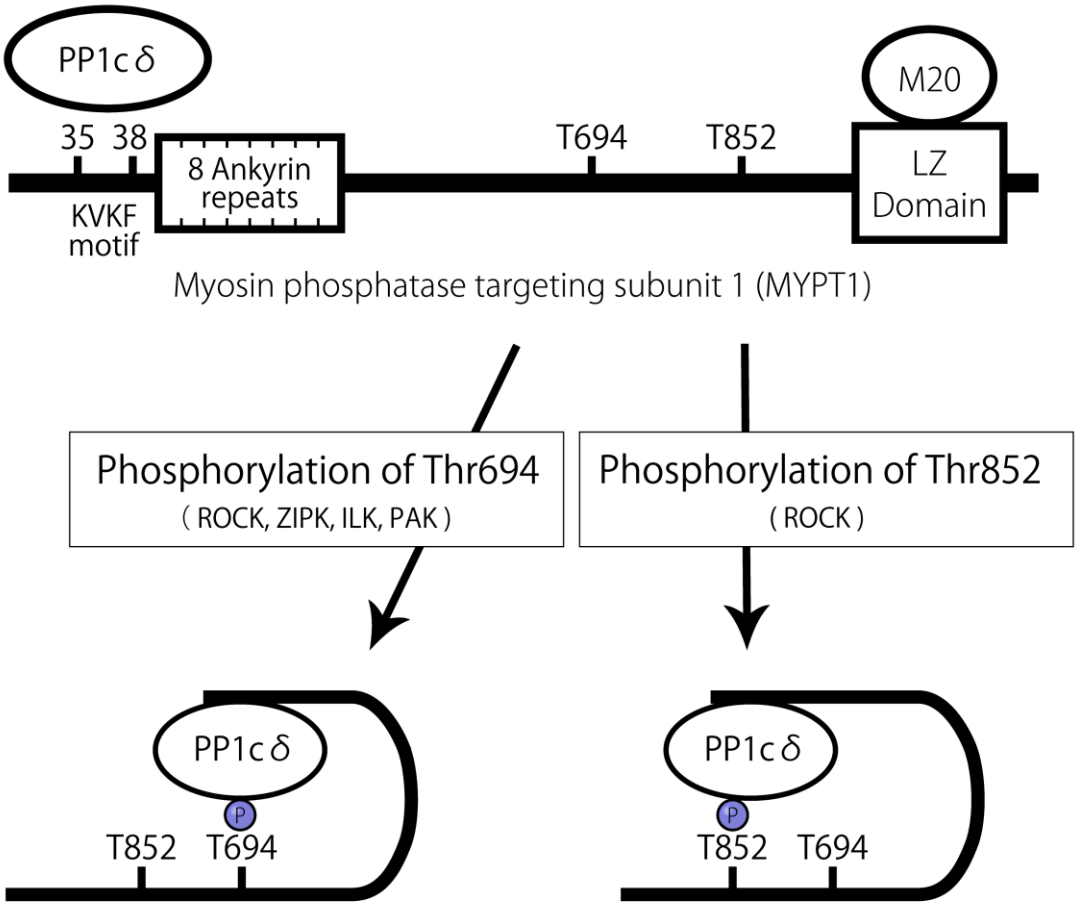

Figure 4-1. The domain structure and autoinhibition of myosin phosphatase (MLCP) The catalytic subunit (PP1cδ) is associated with N-terminal KVKF motif in MYPT1. The N-terminal 8 ankyrin repeats domain may bind to the phosphorylated MRLC. With unphosphorylated MYPT1, the PP1cδ is accessible to the phospho-MRLC. Upon the phosphorylation of Thr694 or Thr852, the phosphorylation site directly interact with the active site of PP1 and suppresses the phosphatase activity.

4.2 Results

4.2.1 Involvement of MLCP with compressive-induced MRLC dephosphorylation

We examined the role of MLCP in MRLC dephosphorylation as a response to compressive loading. First, the catalytic activity of MLCP was inhibited with calyculin A, a PP1 and PP2A inhibitor. Cells were treated with calyculin A (2 nM) 90 minutes before compressive loading, and then we examined whether MRLC was dephosphorylated in response to compressive stress (Figure 4-2A). Accordingly, when compression was applied to cells under the treatment of calyculin A, MRLC was not dephosphorylated. Next, MYPT1, which is a subunit of MLCP was knocked down using RNAi (Figure 4-2B). As a result, compression did not induce MRLC dephosphorylation in cells transfected with MYPT1 siRNA. Thus, these results suggested that MLCP activity was involved in MRLC dephosphorylation in response to compression.

4.2.2 Dephosphorylation of MYPT1 (Thr852) in response to compressive loading

In order to reveal how the MLCP is activated after cell compression, we investigated the phosphorylation levels of MYPT1. MYPT1 (Thr852) was significantly dephosphorylated after cell compression, whereas MYPT1 (Thr694) was not. These findings indicate that compression activated MLCP via MYPT1 (Thr852) dephosphorylation, which resulted in the dephosphorylation of MRLC. The Thr694 site of MYPT1 is phosphorylated by various kinases: ROCK, ZIPK, ILK, and PAK (Kiss *et al*., 2002; Takizawa *et al*., 2002; Hudson *et al*., 2012). On the other hand, the Thr852 site of MYPT1 is phosphorylated only by ROCK (Hudson *et al*., 2012). Taken together, it may be suspected that ROCK was inactivated by compressive stress.

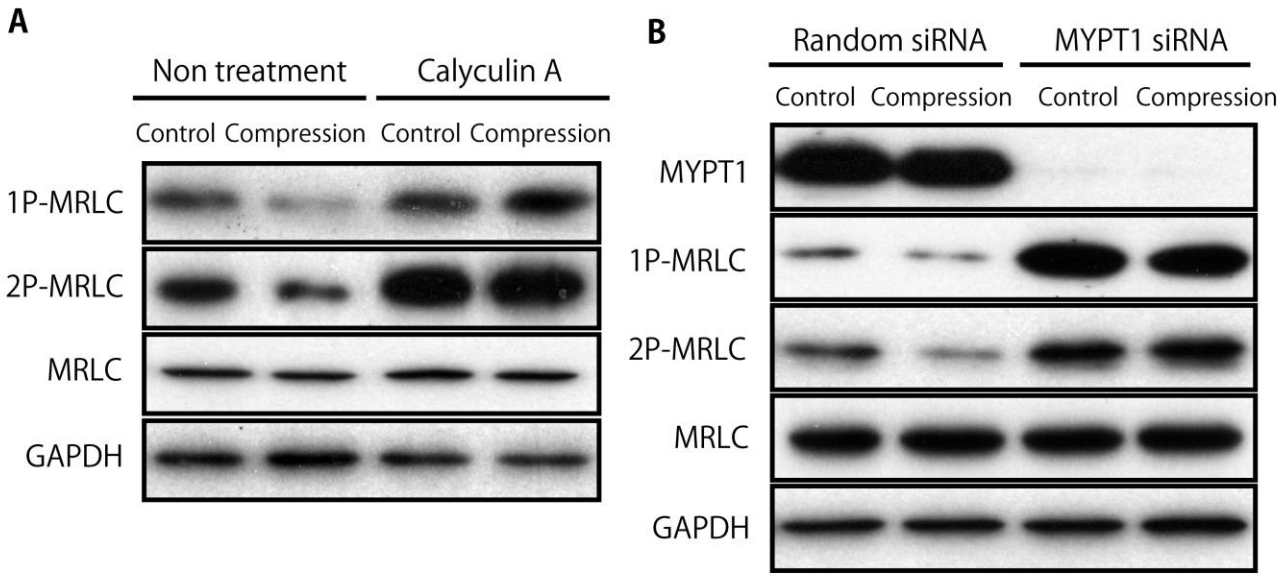

Figure 4-2. Compression induced inactivation of ROCK, and activated MLCP.

(A) Influence of MLCP inhibition on phosphorylated MRLC under compressive stimulation. Cells were compressed 90 minutes after the treatment of calyculin A (2 nM). Uncompressed cells were used as a control, and compressed samples were taken from cells 5 minutes after compression.

(B) Effect of siRNA-mediated knockdown of MYPT1 on phosphorylated MRLC under compressive loading. Cells were transfected with random or MYPT1 siRNA 24 hours before cell compression. 1P-MRLC, 2P-MRLC, and GAPDH were measured by western blotting.

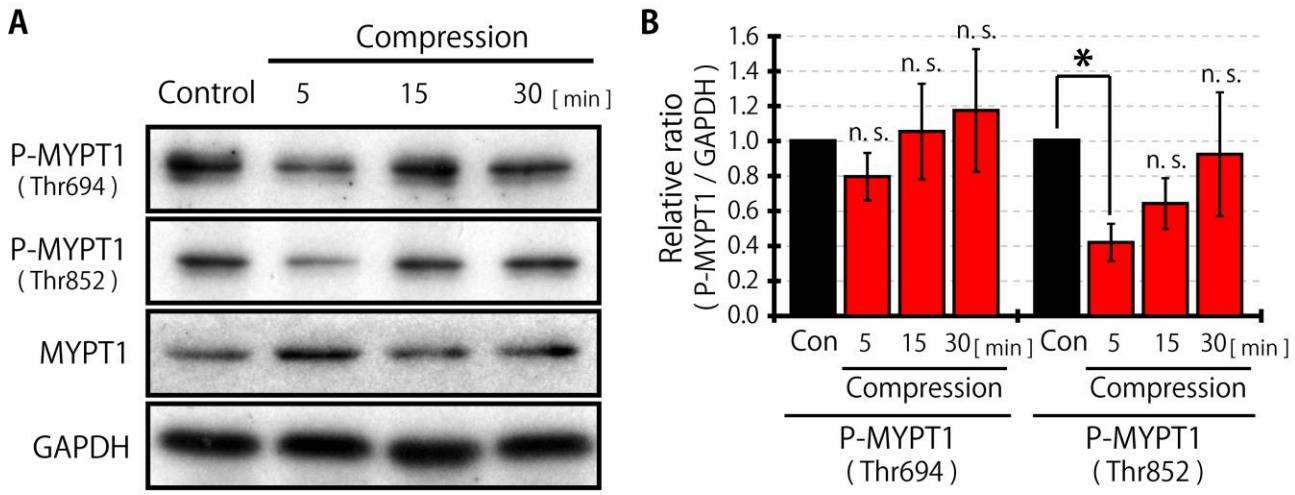

Figure 4-3. The phosphorylation levels of MYPT1 after compressive loading

(A) Western blotting for phosphorylated MYPT1 under cell compression. MYPT1 (Thr696) and MYPT1 (Thr853) dephosphorylation 5 minutes after cell compression were detected by western blotting.

(B) Quantative analysis of the phosphorylation levels of MYPT1. The levels of phospho-MYPT1 and GAPDH were quantified with Image J software. Quantification of western blots represents an average of three independent experiments, mean ± SEM. *, $p < 0.05$. n. s. stand for non significant difference between control and compression sample.

Chapter 5

RhoA activation and phosphorylation by compressive loading

5.1 Introduction

5.1.1 Rho-associated coiled-coil containing protein kinase (ROCK)

It was deduced that ROCK was inactivated in response to compressive loading. ROCK is a serine/threonine protein kinase. ROCK is composed of a N-terminal kinase domain, a central coiled-coil-forming region and a C-terminal pleckstrin homology (PH) domain (Figure 5-1A) (Fujisawa *et al*., 1996). The coiled-coil region has a Rho-binding domain, and PH domain has a cysteine-rich domain. The C-terminal region containing the Rho-binding and PH domains can bind to the N-terminal kinase region and decreases the kinase activity of ROCK (Figure 5-1B) (Amano *et al*., 1999). Thus, the segment is called an autoinhibitory region. This autoinhibitory interaction is disrupted by binding of GTP-bound RhoA (active form) to the Rho-binding domain in ROCK (Ishizaki *et al*., 1996).

5.1.2 RhoA

A small GTPase protein RhoA is a member of Ras superfamily including Rac and Cdc42. RhoA was involved in many cellular function such as contractile force generation, cell cycle progression, transcriptional control and matrix remodeling

(Etienne-Manneville and Hall. 2002). RhoA takes two forms: an active GTP-bound and an inactive GDP-bound state (Figure 5-2). These states change through nucleotide exchange and own GTPase activity. Some proteins are associated with the regulation of RhoA activity. Guanine nucleotide exchange factors (GEFs) can replace GDP binding to inactive RhoA with GTP and activate RhoA (Bos *et al*., 2007). GTPase activating proteins (GAPs) stimulate GTP hydrolysis activity of RhoA, which resulted in inactivation of RhoA (Bos *et al*., 2007). Rho guanine-dissociation inhibitors (RhoGDIs) form a complex by binding to GDP-bound RhoA (inactive form) and extract RhoA from membrane where it can interact with its effectors (Dovas and Couchman, 2005). The complex also inhibits nucleotide exchange and GTPase activity of RhoA by preventing interaction between RhoA and GEF/GAP proteins.

RhoA phosphorylation was also involved with regulation of RhoA signaling. Protein kinase A (PKA) phosphorylates GTP-bound RhoA on Ser188 (Lang *et al*., 1996). PKA-mediated RhoA phosphorylation enhanced the interaction between RhoA and RhoGDI, and thereby promotes for RhoGDIs to release RhoA from membrane (Lang *et al*., 1996). Interestingly, phosphorylation of RhoA affects binding affinity of RhoA to the effectors. Nusser *et al*. reported that phosphorylated RhoA (Ser188) cannot bind to ROCK, whereas it can interact with PKN, mDia1 and Rhotekin. Thus, RhoA phosphorylation inhibits RhoA/ROCK signaling pathway.

5.1.3 Adenylyl cyclase/cAMP/protein kinase A

Protein kinase A (PKA) is a serine/threonine kinase activated dependently on intracellular concentration of cyclic AMP (cAMP). PKA is composed of two catalytic subunits and two regulatory subunits (Figure 5-3) (Edelman *et al*., 1987). Regulatory subunits eclipse active sites of catalytic subunits. When cAMPs increases and binds to regulatory subunits, regulatory subunits release the catalytic subunits, which resulted in PKA activation (Shabb, 2001).

cAMP is produced from ATP by an adenylyl cyclase. Adenylyl cyclases are twelve-transmembrane protein consisting of two transmembrane regions and two cytoplasmic regions (Tesmer and Sprang, 1998). The transmembrane regions function as membrane localization. The cytoplasmic regions are composed of catalytic apparatus and several regulatory sites. Adenylyl cyclases have ten isoforms. The activities of adenylyl cyclases are regulated by multiple factors (Cooper, 2005; Sunahara and Taussig, 2002; Willoughby and Cooper, 2007). Gαs subunits of heterotrimeric G proteins stimulate nine types, and Gαi subunits of G proteins inhibit six types. Three types of adenylyl cyclases are activated by calcium ion and other three types are inhibited. PKA and PKC also regulate some adenylyl cyclases.

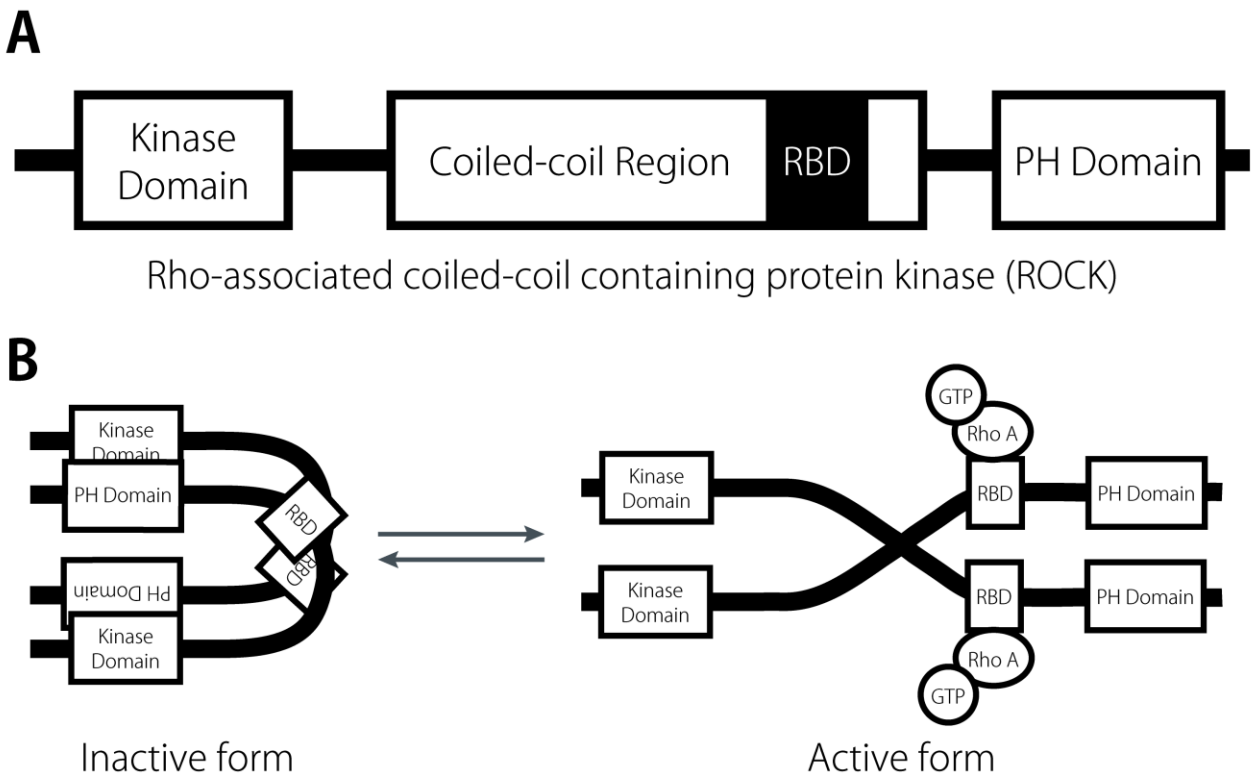

Figure 5-1. The domain structure and regulation of ROCK

(A) The domain structure of ROCK. The kinase domain of ROCK is located in the amino terminus. The sequence of the Rho-binding domain (RBD) is included in the coiled-coil region. In the carboxyl terminus of ROCK, there is a pleckstrin homology (PH) domain.

(B) Conversion of ROCK structure between inactive and active form. In the inactive form, the PH domain and the RBD of ROCK bind to the amino-terminal region, which results in covering catalytic region and suppresses the kinase activity. Binding of GTP-bound RhoA to the RBD activates the ROCK via conformation change of ROCK from the close to the open state.

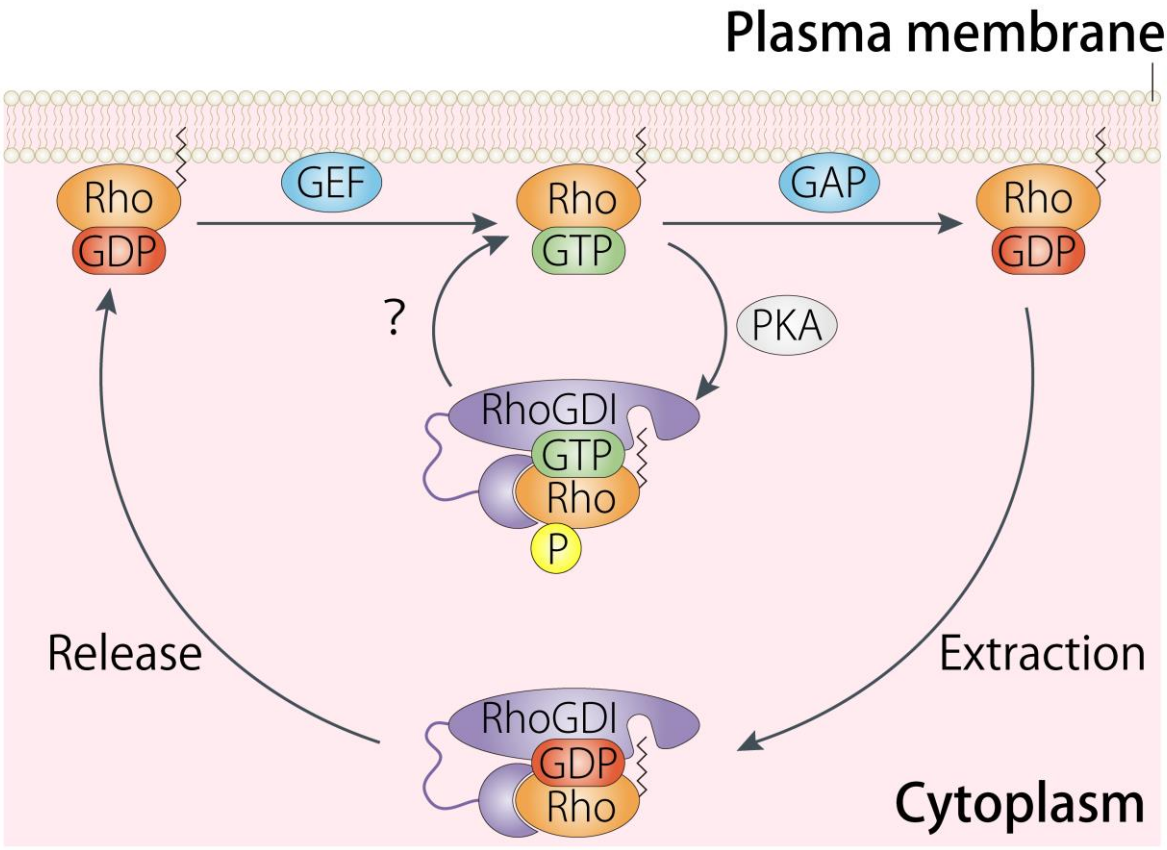

Figure 5-2. Regulating Rho-GTPase activity (Garcia-Mata *et al.*, 2011; Liu *et al.*, 2012)
When RhoA is bound to GTP, the RhoA can bind to and activate its effectors. GTPase-activating proteins (GAPs) stimulate the relatively slow intrinsic GTPase activity of RhoA to promote GDP-bound forms, which results in inactivation of RhoA. Guanine nucleotide-dissociation inhibitors (GDIs) bind the C-terminal isoprenyl moiety of GDP-bound RhoA to separate them from the plasma membrane. Guanine nucleotide-exchange factors (GEFs) catalyse the exchange of GDP for GTP. Protein kinase A phosphorylates Ser188 in RhoA. The GDIs can interact with phosphorylated RhoA regardless of GTP-bound form, resulting in sequestration of GTP-bound RhoA in the cytosol.

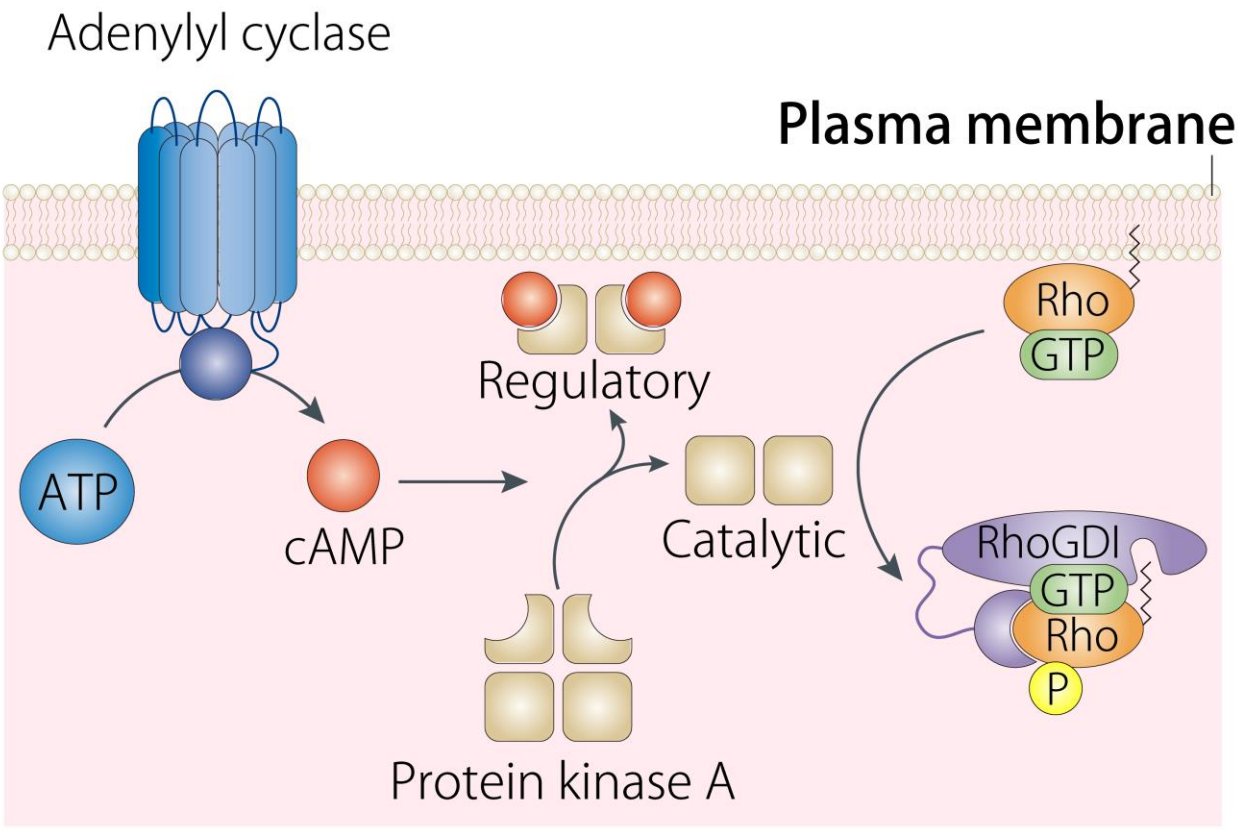

Figure 5-3. Adenylyl cyclase, cAMP, and protein kinase A pathway (Pierre *et al.*, 2009)
Adenylyl cyclase is an transmembrane enzyme that catalyses the synthesis of cAMP from ATP. Adenylyl cyclase is regulated by various factors such as G proteins and calcium ion. Protein kinase A (PKA) is a cAMP-dependent protein kinase. The PKA is a tetrameric complex consisting of two regulatory subunits and two catalytic subunits. Catalytic subunits are bound and inhibited by regulatory subunits. By the binding of two cAMPs to regulatory subunits, the binding affinity of regultory subunits to catalytic subunits decreases. Thus, PKA is then activated.

5.2 Results

5.2.1 RhoA activity and phosphorylation levels after compressive loading

We examined whether compression induced inactivation of RhoA. An immunoprecipitation technique with Rhotekin-RBD beads was used to detect the levels of RhoA-GTP (active RhoA) before and after cell compression. Interestingly, active RhoA was increased 1 minute after compressive stress (Figure 5-4A). Here, there was a discrepancy between inactivated ROCK and activated RhoA after compression. We hypothesized that RhoA was phosphorylated in response to cell compression. Western blot results showed that RhoA (Ser188) was significantly phosphorylated 5 minutes after compressive loading (Figure 5-4B).

5.2.2 Involvements of adenylyl cyclase and protein kinase A (PKA) with compression-induced MRLC dephosphorylation

We investigated the contribution of RhoA phosphorylation by PKA to the MRLC dephosphorylation response. First, we examined the efffects of PKA inhibitor H-89

on the phosphorylation levels of RhoA. Cells on a plastic dish were treated with H-89 at a concentration of 30 μM for 90 minutes, and then, phosphorylation levels of RhoA was decreased by H-89 treatment (Figure 5-5A). Next, we investigated the efects of the treatment of H-89 on compressive-induced RhoA phosphorylation and MRLC dephosphorylation. Cells on a silicone rubber were treated with H-89 (30 μM) 90 minutes before compressive loading. PKA inhibitor H-89 resulted in blockage of RhoA phosphorylation in response to cell compression (Figure 5-5B). Additionally, there was no significant difference between the levels of phosphorylated MRLC in cells with and without compression when treated with PKA inhibitor (Figure 5-5C). Therefore, these results suggest that RhoA phosphorylation induced by PKA leads to MRLC dephosphorylation in response to compressive loading.

The activity of PKA is dependent on intracellular cyclic adenosine monophosphate (cAMP) concentration (Meinkoth *et al*., 1993). cAMP is synthesized from adenosine triphosphate by adenylyl cyclase (Hanoune and Defer, 2001). To examine whether inhibition of adenylyl cyclase suppresses MRLC dephosphorylation in response to compressive loading, we initially investigated the effects of adenylyl cyclase inhibitor (SQ22,536) on the phosphorylation levels of

RhoA. When cells were treated with 100 μM SQ22,536 for 90 minutes, levels of phosphorylated RhoA were decreased (Figure 5-5A). We subsequently investigated the effects of the inhibition of adenylyl cyclases on compressive-induced RhoA phosphorylation and MRLC dephosphorylation. Cells on a silicone rubber were treated with SQ22,536 (100 μM) 90 minutes before compressive loading. Under the treatment of SQ22,536, phosphorylation levels of RhoA were decreased rather than remaining unchanged by compressive loading (Figure 5-5D). Moreover, inhibition of adenylyl cyclase blocked compression-stimulated MRLC dephosphorylation (Figure 5-5E). These results suggest that the adenylyl cyclase/cAMP/PKA signaling pathway is involved in MRLC dephosphorylation response to compression.

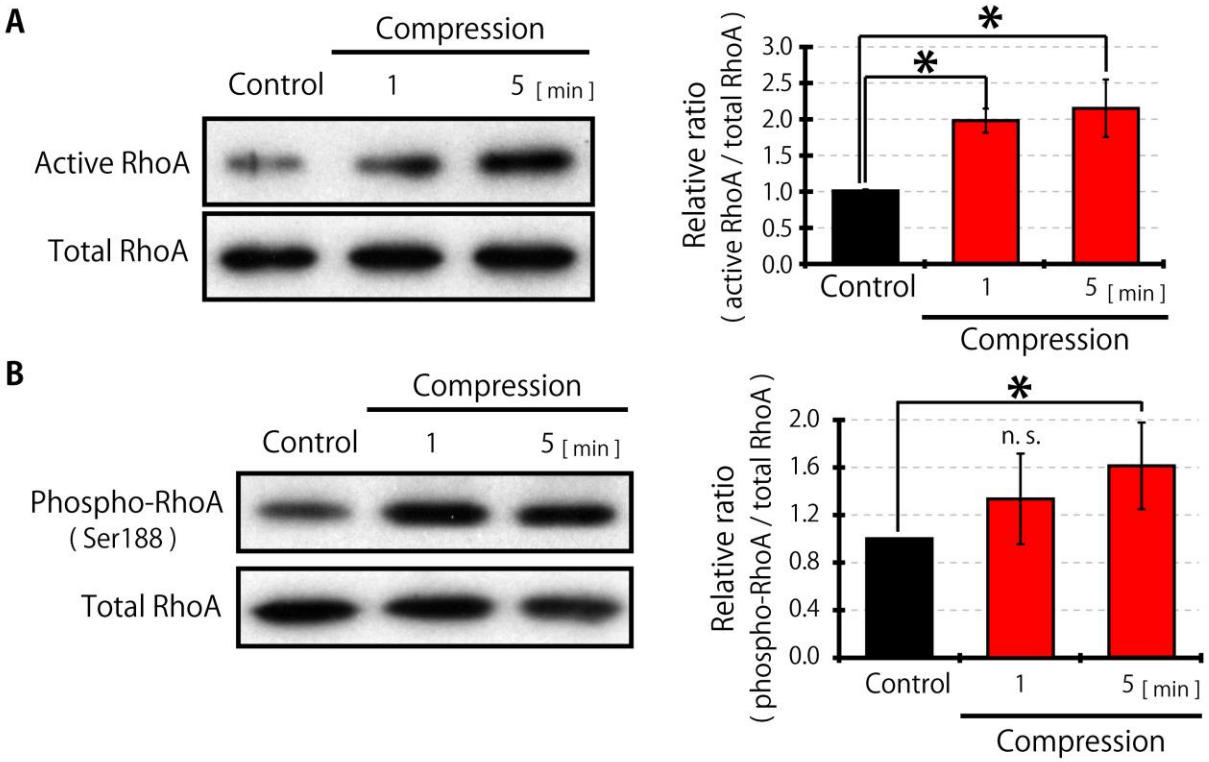

Figure 5-4. Compression induced RhoA activation and phosphorylation.

(A) Detection of active RhoA under compressive loading. Active RhoA (RhoA-GTP) was precipitated with Rhotekin-RBD beads. Total RhoA was used as a loading control.

(B) Western blotting for phosphorylated RhoA after compressing cells. RhoA (Ser188) phosphorylation was detected by western blotting, and total RhoA was used as a loading control. n. s. stand for non significant difference between control and compression sample.

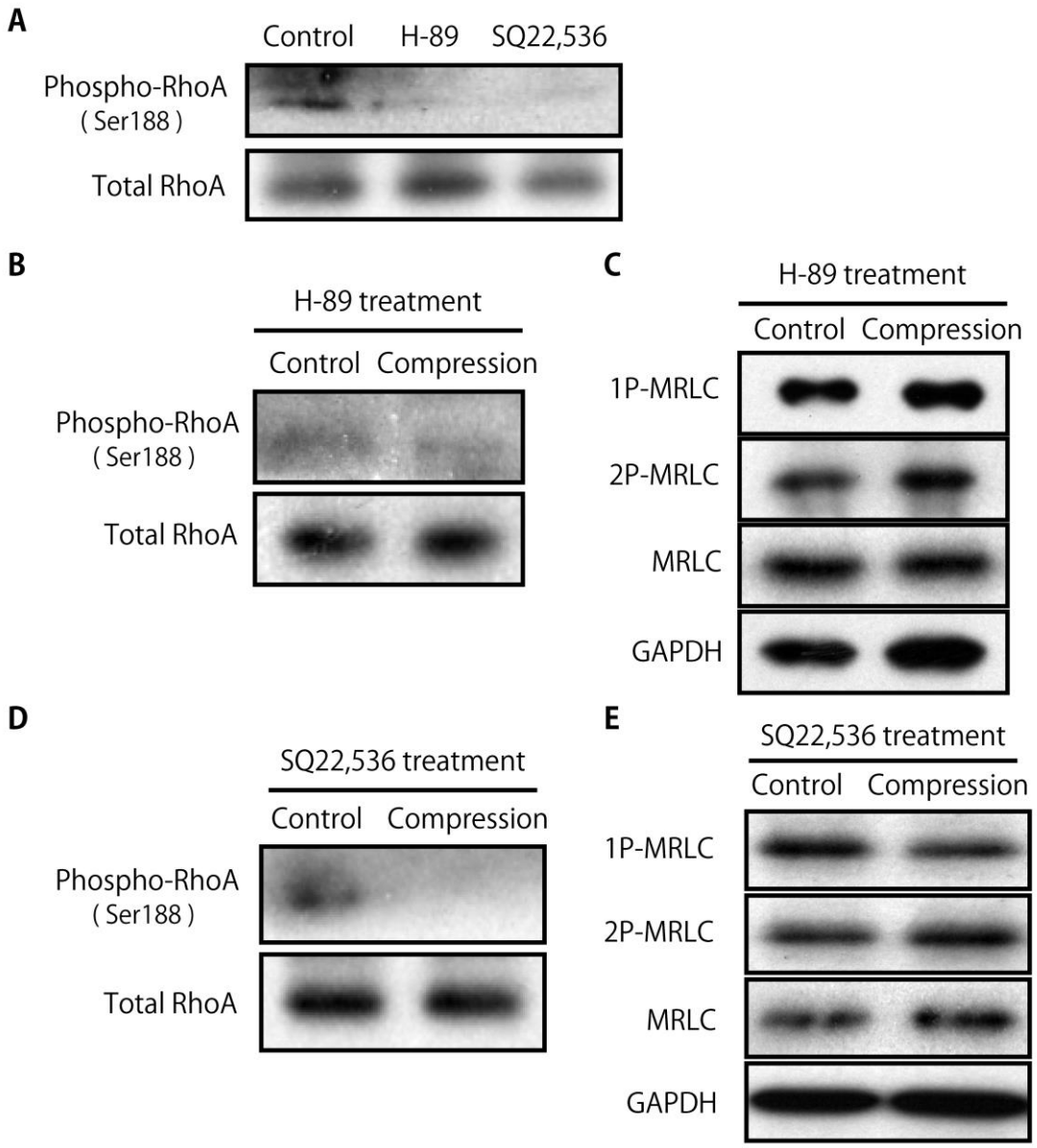

Figure 5-5. The effects of adenylyl cyclase or protein kinase A inhibitor on MRLC dephosphorylation in response to compressive loading

(A) Effects of protein kinase A (PKA) inhibitor H-89 or adenylyl cyclase inhibitor SQ22,536 on phosphorylated RhoA (Ser188). Cells on a plastic dish were treated with 30 μM H-89 or 100 μM SQ22,536 for 90 minutes.

(B), (C) Influence of PKA inhibition on compression-induced RhoA phoshorylation and MRLC dephosphorylation. Cells were compressed under the presence of 30 μM PKA inhibitor H-89.

(D), (E) Effect of inhibition of adenylyl cyclase on compression-stimulated RhoA phoshorylation and MRLC dephosphorylation. Cells were treated with 100 μM adenylyl cyclase inhibitor (SQ22,536) for 90 minutes before cell compression.

Chapter 6

Stretching cells cannot induce phosphorylation of RhoA

6.1 Introduction

6.1.1 Cellular responses to stretching cells

In this study, we investigated mechanism of MRLC dephosphorylation as a response to compressive loading. In order to examine how cells sense differences between stretching and compressing stresses, we checked influences of stretching cells on phosphorylation levels of MRLC.

Our group has studied how cellular stiffness and the phosphorylation levels of MRLC changed in response to stretching cells. In mouse fibroblasts (NIH3T3 cells), MRLC was phosphorylated 15 minutes after cells were uniaxially stretched (Mizutani *et al*., 2009). Cellular stiffness which reflects the strength of cellular tension was increased 10 minutes after cells were stretched (Mizutani *et al*., 2004). The treatment of ROCK inhibitor (Y-27632) blocked stiffening cells as response to stretching. Additionally, the use of dominant negative RhoA (RhoAN19) also inhibited stretch-stimulated increasing cellular stiffness. These results suggested that the increment of cellular stiffness in response to cell stretch was associated with RhoA/ROCK/MRLC signaling pathway.

We checked whether phosphorylation levels of MRLC and RhoA activity were changed by stretching C2C12 cells isotropically. We also investigated effects of stretching cells on phosphorylation levels of RhoA.

6.2 Results

We confirmed effects of stretching stress on phosphorylation levels of MRLC and RhoA activity in C2C12 cells. Mono-phosphorylated MRLC at Ser19 (1P-MRLC) and di-phosphorylated MRLC at Thr18 and Ser19 (2P-MRLC) were detected by western blot at 5 minutes after stretching cells. The levels of phosphorylated MRLC at 5 minutes after stretching increased relative to the control without stretching stress as well as NIH3T3 cells (Figure 6A). The level of GTP-bound RhoA (active RhoA) was obtained by the use of immunoprecipitation technique with Rhotekin-RBD beads at 5 minutes after C2C12 cells were stretched. Then RhoA was activated by stretching C2C12 cells (Figure 6B). Combined with the result that RhoA activation was induced by compressive loading, RhoA was activated in response to both stretching and compressing stress. In other words, it suggests that RhoA cannot distinguish stretching cells from compressive loading. We hypothesized that MRLC dephosphorylation response to cell compression as distinguished from stretching was caused by RhoA phosphorylation, but not due to change in RhoA activity. Western blotting for phosphorylated RhoA was used to examine whether phosphorylated RhoA changed in response to stretching cells. There was no significant difference in RhoA phosphorylation between stretched and unstretched

cells (Figure 6C). Therefore, RhoA phosphorylation may be the means by which MRLC can discriminate between stretched and compressed cells.

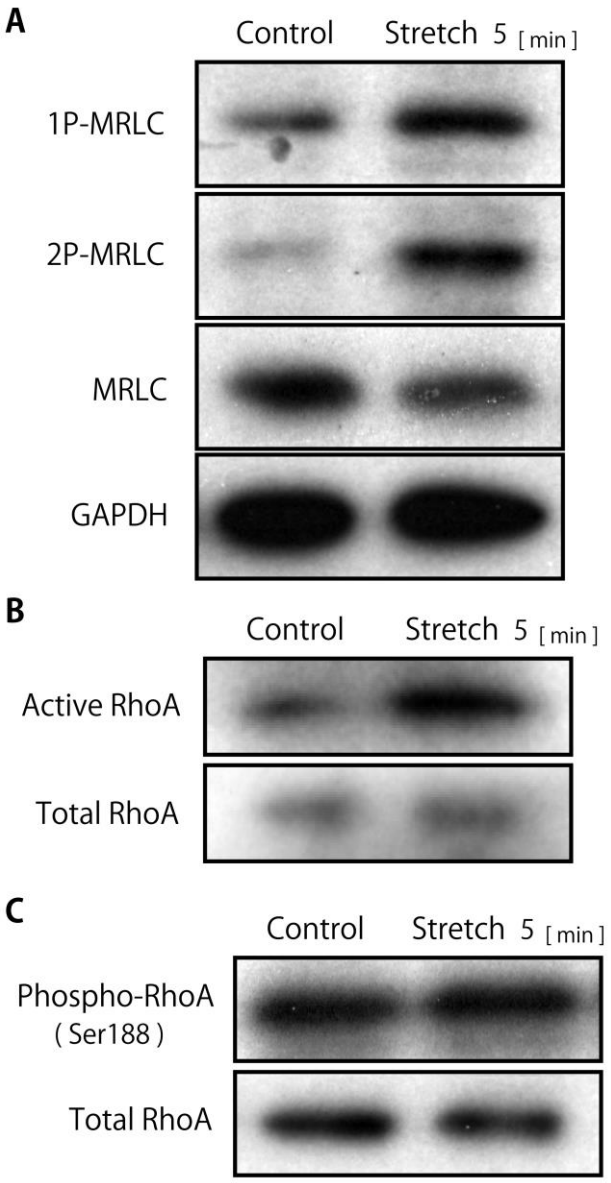

Figure 6. Stretching cells did not affect phosphorylation of RhoA.

(A) Influence of stretching C2C12 cells on phosphorylation of MRLC. MRLC phosphorylation 5 minutes after cell stretching was monitored by western blotting. GAPDH was used as a loading control.

(B) Effects of stretch stress on RhoA activity. Active RhoA (RhoA-GTP) and total RhoA after 5 minutes of cell stretching were detected by western blotting.

(C) Detection of phosphorylated RhoA under cell stretching. Phospho-RhoA and

Chapter 7

Discussion

In this study, we obtained the following results. (1) Myosin regulatory light chain (MRLC) was dephosphorylated in C2C12 cells subjected to compressive loading. (2) F-actin is not affected by compressive loading (14%). (3) MRLC dephosphorylation in response to cell compression was induced by MLCP activation via MYPT1 (Thr853) dephosphorylation. (4) Compression may induce ROCK inactivation despite RhoA activation. (5) The MRLC dephosphorylation response was due to RhoA phosphorylation through the adenylyl cyclase/protein kinase A signaling pathway. Figure 7-1 is the signaling pathway summarizing the results suggested in the present work. Additionally, we hypothesize that RhoA phosphorylation is also an important process for distinguishing between stretching and compressing cells.

The finding that MRLC was dephosphorylated in response to compressive loading is thought to influence cell density. Keeping the cell density constant can help control tissue and organ size, and aberration of this system can trigger cancer development and other diseases. An increase in cell density due to excess cell division causes compressive stress on the cells themselves. In order to reduce the excessive cell density, cells must stop proliferating. Recently, it was reported that cells on a stiffer extracellular matrix (ECM) activate Yes-associated protein (YAP) and transcriptional coactivator with PDZ-binding motif (TAZ), which promotes cell

proliferation and cell survival (Dupont *et al*., 2011). YAP/TAZ activation in response to ECM stiffness was mediated by MRLC phosphorylation. Thus, the MRLC dephosphorylation response to compression may inhibit cell proliferation signaling via YAP/TAZ. This suggestion is supported by the report that DNA synthesis scaled directly with projected cell area: cells on a small adhesive island coated with fibronectin showed low ability of cell proliferation and survival (Chen *et al*., 1997). Additionally, George T. Eisenhoffer reported that increased density in MDCK cells was de-escalated through apical extrusion of cells and returned to the constant cell area (Eisenhoffer *et al*., 2012). Suspension of cell division through YAP/TAZ inactivation and apical extrusion of cells by compressive loading may regulate cell density *in vivo*.

We considered the effect of compressive loading on cell area. Cells can control their own size, and regulate their cell area to keep it constant. For example, immediately following cell division cells are very small, and then gradually grow to the size of their parent cell (Norman *et al*., 2010). We examined how cell size changes in response to compressive loading when cells are forced to decrease in size. As a result, cells gradually grew to a large size after compressive stress and returned to their original size 20 minutes after cell compression (Figure 7-2A). Initially, we

thought that increasing cell size after compressive loading was due to MRLC dephosphorylation. However, cell area is regulated by cellular tension, which is dependent on the phosphorylation of MRLC, and time-dependent change of phosphorylated MRLC in response to compressive loading is correlated with the change in traction force during cell spreading (Dubin-Thaler *et al*., 2008). Therefore, we investigated the cell area of cells that were compressed under the inhibition of adenylyl cyclase, which is important in the MRLC dephosphorylation response to compression. However, cells under the treatment of adenylyl cyclase inhibitor also return to their original size after compressive loading along with the non-treated cells (Figure 7-2B,C). Thus, these results suggested that MRLC dephosphorylation by cell compression may not be necessary to regulate cell area.

Cell spreading is promoted by protrusion of membrane ruffles. Rho GTPases is implicated in the formation of actin filamients in membrane protrusion. A recent study showed that Rac1, which is one of the RhoGTPases, was essential for cell migration, but not for cell spreading (Steffen *et al*., 2013). On the other hand, RhoA is involved not only in contractile force generation by ROCK, but also membrane protrusion by mDia1. Using a FRET technique, it was reported that RhoA was activated 40 seconds before Rac1 activation in lamellipodia formation (Machacek *et*

al., 2009). Therefore, the RhoA/mDia1 signaling pathway may be related to reconstruction of cell area after compressive loading.

Based on Figure 3-1 and 3-2, we concluded that compressive loading did not induce collapse or thickness change of actin filaments. However, actin particles with approximately 0.5 μm diameter were observed after cell compression (Fig. 3-2A). There are three conceivable causes why the actin particles were generated. (i) Cortical thinner actin filaments may be disrupted. Hayakawa *et al*. reported that actin-severing protein cofilin selectively bind to unstrained actin fibers. Since compressive loading decreased tension of actin fibers, enabling binding of cofilin to the the actin fibers and sebsequently severing them. Although disruption of actin fibers was not observed with live-cell imaging, observable actin fibers using this technique are thick bundles of actin filaments called stress fibers. Thus, thinner cortical actin filaments may be disrupted by cofilin, so that actin particles increased after cell compression. (ii) The actin particles are possibly the nucleus of actin polymerization. Compressive loading induced RhoA activation and can activate mDia1. mDia1 can stabilize actin dimers and trimers that are intermediates of acin polymerization (Moseley *et al*., 2006). Profilin interacts with mDia1 and recruits the actin monomers to the actin nucleus, therefore, actin filaments are elongated (Kovar

et al., 2006). RhoA activation by compressive stress might induce activation of mDia1, resulting in nucleation of actin polymerization. (iii) The particles may be endosomes and exosomes. Endocytosis and exocytosis regulate not only composition and surface area, but also tension of cellular membranes. Endocytosis increases membrane tension by removing excess membrane components, whereas exocytosis relaxes the cell membrane. In this study, compressive loading decreased cellular membrane tension. In order to maintain the plasma membrane tension, endocytosis may be stimulated after cell compression. Additionally, clathrin-mediated endocytosis is associated with the actin cytoskeleton. Actin dynamics is required for membrane invagination and clathrin-mediated plaque uptake (Salisbury *et al*., 1980). Actin and some of its interacting proteins (Arp2/3, cortactin, Hip1R etc.) are recruited to clathrin-containing structures upon scission from the plasma membrane (Le Clainche *et al*., 2007; Merrifield *et al*., 2004). Hence, it would not be surprising if endocytosis was activated by change in the tension of the actin cytoskeleton after cell compression.

In this study, RhoA was activated after induction of compressive stimuli (Figure 5-4A). Furthermore, a previous study revealed that stretching cells also induced RhoA activation (Mizutani *et al*., 2009). In summary, cells cannot sense

differences between compressing and stretching cells in terms of RhoA activity. Some guanine nucleotide exchange factors (GEF), which are activators for RhoA, are known to respond to mechanical stress. For example, LARG and GEF-H1 were activated in response to generate tensile forces on fibronectin-coated magnet beads attached to the dorsal surface of cells (Guilluy *et al*., 2011). Vav-2 which can exchange GDP for GTP on several Rho-GTPases including RhoA, Rac1, RhoG, and Cdc42 responded to fluid shear flow and ECM stiffness (Liu *et al*., 2013; Hobert *et al*., 1996). Alternatively, p190RhoGEF (Lim *et al*., 2008) and PDZRhoGEF (Iwanicki *et al*., 2008), also known as RhoGEFs, were activated by mechanical stress. These RhoGEFs may sense compressive stress and activate RhoA.

This study reported that adenylyl cyclase was involved with MRLC dephosphorylation in response to compressing cells (Figure 5-5E). Ten types of adenylyl cyclases have been found, of which eight types are expressed in mouse. Adenylyl cyclase activity is altered by some agents. All adenylyl cyclase isozymes are stimulated by forskolin (Pinto *et al*., 2008), seven types are regulated by protein kinase A and C (Tian and Laychock. 2001), and three types are activated by Ca^{2+} or calmodulin (Halls and Cooper. 2011). Additionally, cytoskeleton disruption also enhanced some adenylyl cyclases (Grunspan-Swirsky and Pick.

1978). A previous study revealed that adenylyl cyclase type 6, which is activated only by forskolin, was mechanoresponsive factor that increased inside the cells in response to shear stress (Kwon *et al*., 2010). However, it has not been reported that compression induced forskolin products or increased intracellular Ca^{2+}. We did not observe collapse of actin fibers (Figure 3-1 and 3-2) or an increase in intracellular Ca^{2+} after compressive loading to cells (data not shown). Further work is needed to investigate which adenylyl cyclases are activated in response to compressive loading.

Lastly, we note the specificity of the PKA inhibitor H-89. H-89 is currently used as a selective and potent inhibitor of protein kinase A (PKA). However, Davies *et al.* reported that H-89 inhibits at least eight kinases except for PKA. It is also noted that ROCK is included in the kinases targeted by H-89. Thus, inhibition of other kinases excluding PKA (especially ROCK) may affect dephosphorylation of MRLC in response to compressive loading. Nevertheless, H-89 blocked phosphorylation of RhoA after cell compression. Within the targets of H-89, the only kinase that can regulate phosphorylation levels of RhoA is PKA. It was reported that phosphorylation of RhoA induces ROCK inactivation and affects the phosphorylation levels of MRLC (Aburima *et al*., 2013). Additionally, SQ22,536 also

prevented RhoA phosphorylation and MRLC dephosphorylation in response to compressive loading (Figure 5-5D and 5-5E). SQ22,536 inhibits some adenylyl cyclases, which results in inhibition of cAMP formation and PKA activity. Hence, we concluded that the adenylyl cyclase/cAMP/PKA signaling pathway is involved in compression-induced MRLC dephosphorylation.

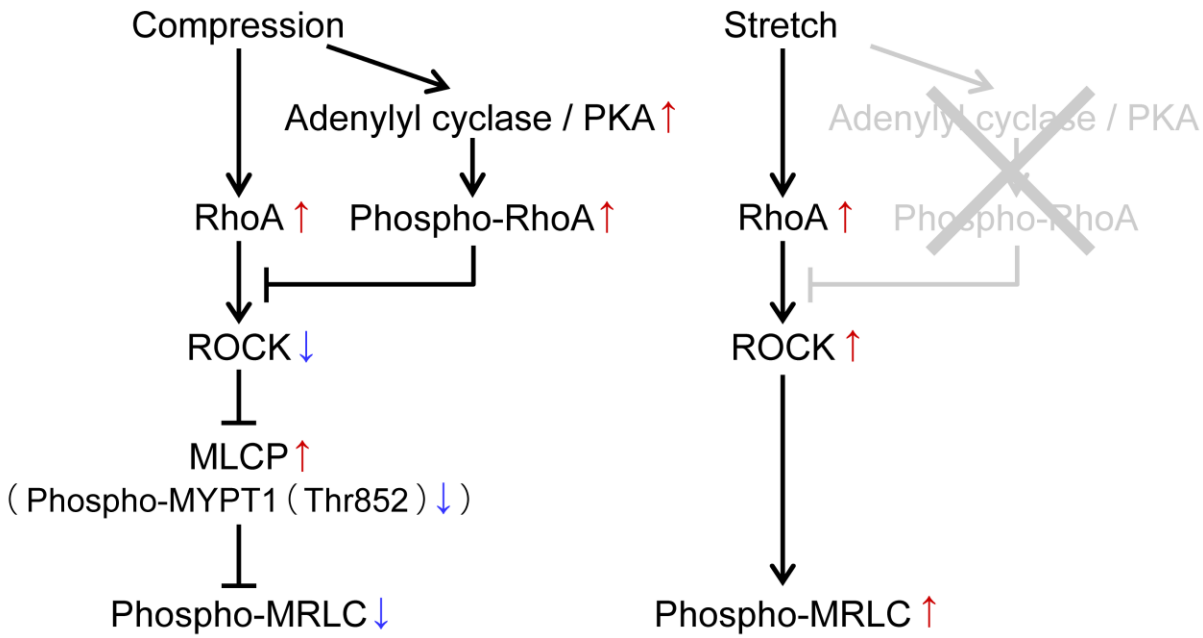

Figure 7-1. Proposed model for compression-induced dephosphorylation of myosin regulatory light chain (MRLC).

In C2C12 cells subjected to compressive loading, RhoA and adenylyl cyclase activation were induced. Adenylyl cyclase activation may activate protein kinase A (PKA) via cAMP production. RhoA phosphorylation by PKA induces decreasing affinity of RhoA for ROCK and inactivates ROCK (Nusser *et al.*, 2006). Myosin phosphatase target subunit 1 (MYPT1) at Thr852 which is kinase substrate of ROCK is dephosphorylated. Accordingly, myosin phosphatase (MLCP) is activated and dephosphorylates MRLC. Right pathway is the signaling pathway of MRLC phosphorylation as response to cell stretching.

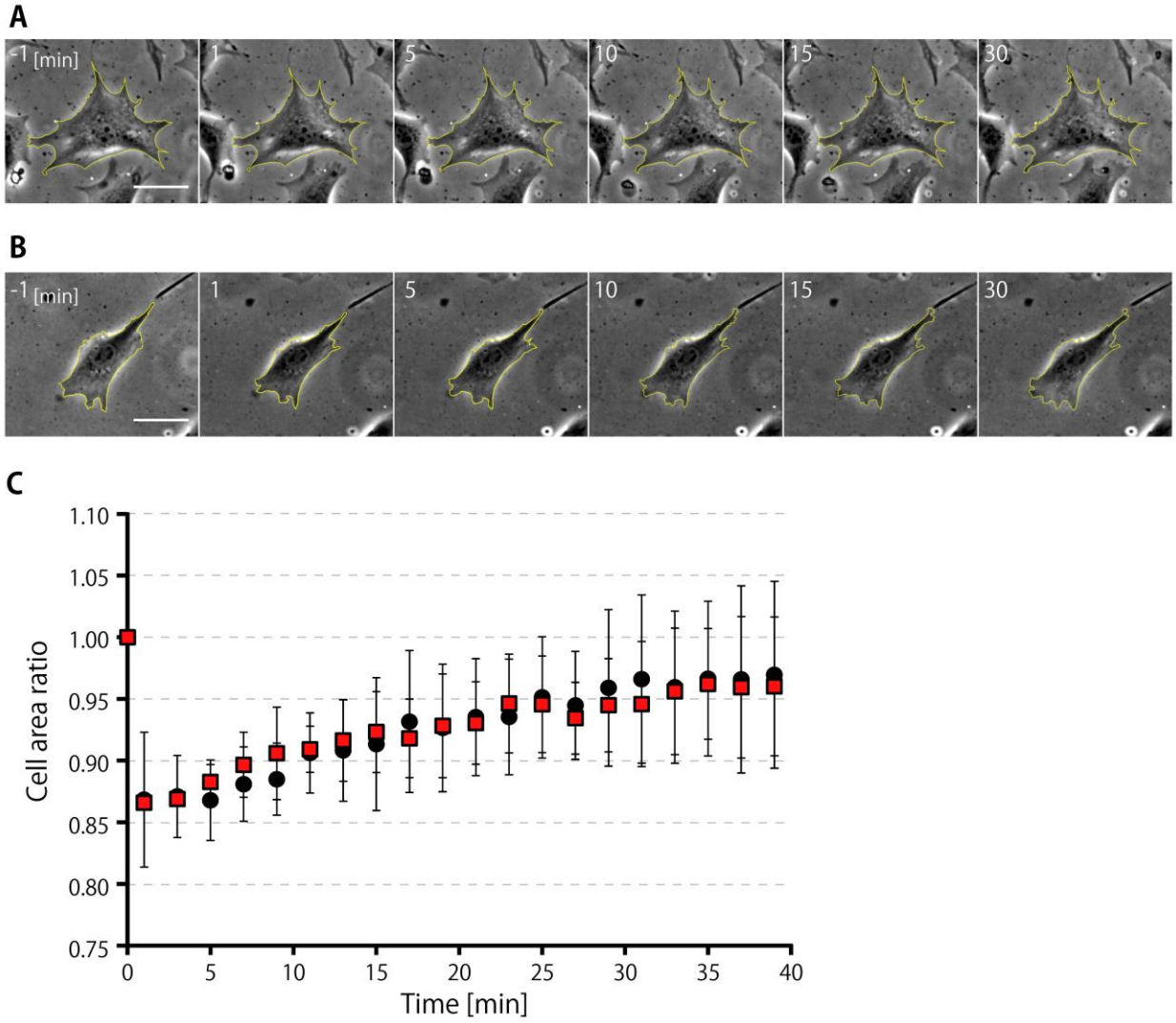

Figure 7-2. Cell area homeostasis in response to compressive loading, is not dependent on adenylyl cyclase.

Phase-contrast imaging was performed to examine the change in cell area after cell compression. Figures show a representative single cell before and after compressive strain for non-treatment (A) and under the treatment of adenylyl cyclase inhibitor (SQ22,536) (B). The yellow line shows the perimeter region of the cell. Numbers in upper left of the images are relative time (min) from the onset of compressive loading. Scale bar is 50 μm. (C) Quantitative analysis of cell area after cell compression. Cell area relative to the cell area before compressive loading was plotted. The black circles indicate the cell area under the non-treatment, and the red squares indicate the cell area under the treatment of SQ22,536. Quantification of cell area represents an average of 3 independent experiments including 12 individual cells, mean ± SEM.

References

Aburima A, Wraith KS, Raslan Z, Law R, Magwenzi S, Naseem KM. (2013) cAMP signaling regulates platelet myosin light chain (MLC) phosphorylation and shape change through targeting the RhoA-Rho kinase-MLC phosphatase signaling pathway. Blood 122: 3533-3545.

Alessi D, MacDougall LK, Sola MM, Ikebe M, Cohen, P. (1992) The control of protein phosphatase-1 by targeting subunits. The major myosin phosphatase in avian smooth muscle is a novel form of protein phosphatase-1. Eur J Biochem 210: 1023-1035.

Amano M, Chihara K, Nakamura N, Kaneko T, Matsuura Y, Kaibuchi K. (1999) The COOH terminus of Rho-kinase negatively regulates rho-kinase activity. J Biol Chem. 274: 32418-32424.

Bathe M, Heussinger C, Claessens MM, Bausch AR, Frey E. (2008) Cytoskeletal bundle mechanics. Biophys J. 94: 2955-2964.

Bos JL, Rehmann H, Wittinghofer A. (2007) GEFs and GAPs: critical elements in the control of small G proteins. Cell. 129: 865-877.

Chen CS, Mrksich M, Huang S, Whitesides GM, Ingber DE. (1997) Geometric

control of cell life and death. Science 276: 1425-1428.

Cooper DM. (2005) Compartmentalization of adenylate cyclase and cAMP signalling. Biochem. Soc. Trans. 33: 1319–1322.

Coste B, Mathur J, Schmidt M, Earley TJ, Ranade S, Petrus MJ, Dubin AE, Patapoutian A. (2010) Piezo1 and Piezo2 are essential components of distinct mechanically activated cation channels. Science 330: 55-60.

Davies SP, Reddy H, Caivano M, Cohen P. (2000) Specificity and mechanism of action of some commonly used protein kinase inhibitors. Biochem J 351: 95-105.

Dennerll TJ, Joshi HC, Steel VL, Buxbaum RE, Heidemann SR. (1988) Tension and compression in the cytoskeleton of PC-12 neurites. II: Quantitative measurements. J. Cell Biol 107: 665-674

Dovas A, Couchman JR. (2005) RhoGDI: multiple functions in the regulation of Rho family GTPase activities. Biochem J. 390:1-9.

Dubin-Thaler BJ, Hofman JM, Cai Y, Xenias H, Spielman I, Shneidman AV, David LA, Döbereiner HG, Wiggins CH, Sheetz MP. (2008) Quantification of cell edge velocities and traction forces reveals distinct motility modules during cell spreading. PLoS One 3: e3735.

Dupont S, Morsut L, Aragona M, Enzo E, Giulitti S, Cordenonsi M, Zanconato F, Le

Digabel J, Forcato M, Bicciato S, Elvassore N, Piccolo S. (2011) Role of YAP/TAZ in mechanotransduction. Nature 474: 179-183.

Edelman AM, Blumenthal DK, Krebs EG. (1987) Protein serine/threonine kinases. Annu. Rev. Biochem. 56: 567–613.

Ehrlicher AJ, Nakamura F, Hartwig JH, Weitz DA, Stossel TP. (2011) Mechanical strain in actin networks regulates FilGAP and integrin binding to filamin A. Nature. 478: 260-263.

Eisenhoffer GT, Loftus PD, Yoshigi M, Otsuna H, Chien CB, Morcos PA, Rosenblatt J. (2012) Crowding induces live cell extrusion to maintain homeostatic cell numbers in epithelia. Nature 484: 546-549.

Etienne-Manneville S, Hall A. (2002) Rho GTPases in cell biology. Nature. 420: 629-635.

Fujisawa K, Fujita A, Ishizaki T, Saito Y, Narumiya S. (1996) Identification of the Rho-binding domain of p160ROCK, a Rho-associated coiled-coil containing protein kinase. J Biol Chem. 271: 23022-23028.

Garcia-Mata R, Boulter E, Burridge K. (2011) The 'invisible hand': regulation of RHO GTPases by RHOGDIs. Nat Rev Mol Cell Biol. 12: 493-504.

Grunspan-Swirsky A and Pick E. (1978) Enhancement of macrophage adenylate

cyclase by microtubule disrupting drugs. Immunopharmacology 1: 71-82.

Gschwend S, Henning RH, Pinto YM, de Zeeuw D, van Gilst WH, Buikema H. (2003) Myogenic constriction is increased in mesenteric resistance arteries from rats with chronic heart failure: instantaneous counteraction by acute AT1 receptor blockade. Br J Pharmacol 139: 1317-1325.

Guilluy C, Swaminathan V, Garcia-Mata R, O'Brien ET, Superfine R, Burridge K. (2011) The Rho GEFs LARG and GEF-H1 regulate the mechanical response to force on integrins. Nat Cell Biol 13: 722-727.

Halls ML and Cooper DM. (2011) Regulation by Ca^{2+}-signaling pathways of adenylyl cyclases. Cold Spring Harb Perspect Biol 3: a004143.

Hanoune J and Defer N (2001) Regulation and role of adenylyl cyclase isoforms. Annu Rev Pharmacol Toxicol 41: 145-174.

Hara F, Fukuda K, Asada S, Matsukawa M, Hamanishi C. (2001) Cyclic tensile stretch inhibition of nitric oxide release from osteoblast-like cells is both G protein and actin-dependent. J Orthop Res 19: 126-131.

Hartshorne DJ. (1998) Myosin phosphatase: subunits and interactions. Acta Physiol Scand. 164: 483-493.

Hayakawa K, Tatsumi H, Sokabe M. (2011) Actin filaments function as a tension

sensor by tension-dependent binding of cofilin to the filament. J Cell Biol 195: 721-727.

Hernandez OM, Jones M, Guzman G, Szczesna-Cordary D. (2007) Myosin essential light chain in health and disease. Am J Physiol Heart Circ Physiol. 292: H1643-1654.

Hirano K, Phan BC, Hartshorne DJ. (1997) Interactions of the subunits of smooth muscle myosin phosphatase. J Biol Chem 272: 3683-3688.

Hirata N, Takahashi M, Yazawa M. (2009) Diphosphorylation of regulatory light chain of myosin IIA is responsible for proper cell spreading. Biochem Biophys Res Commun. 381: 682-687.

Hobert O, Schilling JW, Beckerle MC, Ullrich A, Jallal B. (1996) SH3 domain-dependent interaction of the proto-oncogene product Vav with the focal contact protein zyxin. Oncogene 12: 1577-1581.

Holmes KC. (2008) Myosin structure. Proteins and Cell Regulation. 7: 35-54

Hudson CA, Heesom KJ, Lopez Bernal A. (2012) Phasic contractions of isolated human myometrium are associated with Rho-kinase (ROCK)-dependent phosphorylation of myosin phosphatase-targeting subunit (MYPT1). Mol Hum Reprod 18: 265-279.

Ichikawa K, Hirano K, Ito M, Tanaka J, Nakano T, Hartshorne DJ. (1996) Interactions and properties of smooth muscle myosin phosphatase. Biochemistry 35: 6313-6320.

Ikebe M and Hartshorne DJ. (1985) Phosphorylation of smooth muscle myosin at two distinct sites by myosin light chain kinase. J Biol Chem 260: 10027-10031.

Ishizaki T, Maekawa M, Fujisawa K, Okawa K, Iwamatsu A, Fujita A, Watanabe N, Saito Y, Kakizuka A, Morii N, Narumiya S. (1996) The small GTP-binding protein Rho binds to and activates a 160 kDa Ser/Thr protein kinase homologous to myotonic dystrophy kinase. EMBO J. 15: 1885-1893.

Iwanicki MP, Vomastek T, Tilghman RW, Martin KH, Banerjee J, Wedegaertner PB, Parsons JT. (2008) FAK, PDZ-RhoGEF and ROCKII cooperate to regulate adhesion movement and trailing-edge retraction in fibroblasts. J Cell Sci 121: 895-905.

Ito M, Nakano T, Erdodi F, Hartshorne DJ. (2004) Myosin phosphatase: structure, regulation and function. Mol Cell Biochem. 259: 197-209.

Izzard AS, Graham D, Burnham MP, Heerkens EH, Dominiczak AF, Heagerty AM. (2003) Myogenic and structural properties of cerebral arteries from the stroke-prone spontaneously hypertensive rat. Am J Physiol Heart Circ Physiol 285:

H1489-1494.

Kawamoto T, Haga H, Tamura K, Mizutani T, Kawabata K. (2008) Mechanical Response to Isotropic Shrinkage of Fibroblasts Measured by Scanning Probe Microscopy. Jpn J Appl Phys 47: 6173-6176

Khromov A, Choudhury N, Stevenson AS, Somlyo AV, Eto M. (2009) Phosphorylation-dependent autoinhibition of myosin light chain phosphatase accounts for Ca^{2+} sensitization force of smooth muscle contraction. J Biol Chem 284: 21569-21579.

Kimura K, Fukata Y, Matsuoka Y, Bennett V, Matsuura Y, Okawa K, Iwamatsu A, Kaibuchi K. (1998) Regulation of the association of adducin with actin filaments by Rho-associated kinase (Rho-kinase) and myosin phosphatase. J Biol Chem 273: 5542–5548.

Kiss E, Muranyi A, Csortos C, Gergely P, Ito M, Hartshorne DJ, Erdodi F. (2002) Integrin-linked kinase phosphorylates the myosin phosphatase target subunit at the inhibitory site in platelet cytoskeleton. Biochemical Journal 365: 79-87.

Kovar DR, Harris ES, Mahaffy R, Higgs HN, Pollard TD. (2006) Control of the assembly of ATP- and ADP-actin by formins and profilin. Cell 124: 423-435.

Krendel M, Mooseker MS. (2005) Myosins: tails (and heads) of functional diversity.

Physiology (Bethesda). 20: 239-251.

Kuo L, Arko F, Chilian WM, Davis MJ (1993) Coronary venular responses to flow and pressure. Circ Res 72: 607-615

Kwon RY, Temiyasathit S, Tummala P, Quah CC, Jacobs CR. (2010) Primary cilium-dependent mechanosensing is mediated by adenylyl cyclase 6 and cyclic AMP in bone cells. FASEB J 24: 2859-2868.

Lang P, Gesbert F, Delespine-Carmagnat M, Stancou R, Pouchelet M, Bertoglio J. (1996) Protein kinase A phosphorylation of RhoA mediates the morphological and functional effects of cyclic AMP in cytotoxic lymphocytes. EMBO J 15: 510-519.

Le Clainche C, Pauly BS, Zhang CX, Engqvist-Goldstein AE, Cunningham K, Drubin DG. (2007) A Hip1R-cortactin complex negatively regulates actin assembly associated with endocytosis. EMBO J 26: 1199-1210.

Lee AA, Delhaas T, McCulloch AD, Villarreal FJ. (1999) Differential responses of adult cardiac fibroblasts to in vitro biaxial strain patterns. J Mol Cell Cardiol. 31: 1833-1843.

Lim Y, Lim ST, Tomar A, Gardel M, Bernard-Trifilo JA, Chen XL, Uryu SA, Canete-Soler R, Zhai J, Lin H, Schlaepfer WW, Nalbant P, Bokoch G, Ilic D, Waterman-

Storer C, Schlaepfer DD. (2008) PyK2 and FAK connections to p190Rho guanine nucleotide exchange factor regulate RhoA activity, focal adhesion formation, and cell motility. J Cell Biol 180: 187-203.

Liu M, Bi F, Zhou X, Zheng Y. (2012) Rho GTPase regulation by miRNAs and covalent modifications. Trends Cell Biol. 22: 365-373

Liu Y, Collins C, Kiosses WB, Murray AM, Joshi M, Shepherd TR, Fuentes EJ, Tzima E. (2013) A novel pathway spatiotemporally activates Rac1 and redox signaling in response to fluid shear stress. J Cell Biol 201: 863-873.

Mabuchi Y, Mabuchi K, Stafford WF, Grabarek Z. (2010) Modular structure of smooth muscle Myosin light chain kinase: hydrodynamic modeling and functional implications. Biochemistry 49: 2903-2917.

Machacek M, Hodgson L, Welch C, Elliott H, Pertz O, Nalbant P, Abell A, Johnson GL, Hahn KM, Danuser G. (2009) Coordination of Rho GTPase activities during cell protrusion. Nature 461: 99-103.

Masumoto A, Mohri M, Shimokawa H, Urakami L, Usui M, Takeshita A. (2002) Suppression of coronary artery spasm by the Rho-kinase inhibitor fasudil in patients with vasospastic angina. Circulation 105: 1545-1547.

Mehta D and Gunst SJ. (1999) Actin polymerization stimulated by contractile

activation regulates force development in canine tracheal smooth muscle. J Physiol 519: 829-840.

Meinkoth JL, Alberts AS, Went W, Fantozzi D, Taylor SS, Hagiwara M, Montminy M, Feramisco JR. (1993) Signal transduction through the cAMP-dependent protein kinase. Mol Cell Biochem 127-128: 179-186.

Merrifield CJ, Qualmann B, Kessels MM, Almers W. (2004) Neural Wiskott Aldrich Syndrome Protein (N-WASP) and the Arp2/3 complex are recruited to sites of clathrin-mediated endocytosis in cultured fibroblasts. Eur J Cell Biol 83: 13-18.

Miyamoto S, Teramoto H, Coso OA, Gutkind JS, Burbelo PD, Akiyama SK, Yamada KM. (1995) Integrin function: molecular hierarchies of cytoskel*et al* and signaling molecules. J Cell Biol 131: 791-805.

Mizutani T, Haga H, Kawabata K. (2004) Cellular stiffness response to external deformation: tensional homeostasis in a single fibroblast. Cell Motil Cytoskeleton 59: 242-248.

Mizutani T, Kawabata K, Koyama Y, Takahashi M, Haga H. (2009) Regulation of cellular contractile force in response to mechanical stretch by diphosphorylation of myosin regulatory light chain via RhoA signaling cascade. Cell Motil Cytoskeleton 66: 389-397.

Moseley JB, Maiti S, Goode BL. (2006) Formin proteins: purification and measurement of effects on actin assembly. Methods Enzymol 406: 215-234.

Nakai K, Hayashi T, Nagaya S, Toyoda H, Yamamoto M, Shiku H, Ikeda Y, Nishikawa M. (1997) Shear stress-induced myosin association with cytoskeleton and phosphorylation in human platelets. Life Sci. 60: PL181-191.

Norman LL, Brugues J, Sengupta K, Sens P, Aranda-Espinoza H. (2010) Cell blebbing and membrane area homeostasis in spreading and retracting cells. Biophys J 99: 1726-1733.

Nusser N, Gosmanova E, Makarova N, Fujiwara Y, Yang L, Guo F, Luo Y, Zheng Y, Tigyi G. (2006) Serine phosphorylation differentially affects RhoA binding to effectors: implications to NGF-induced neurite outgrowth. Cell Signal 18: 704-714.

Oda T, Iwasa M, Aihara T, Maéda Y, Narita A. (2009) The nature of the globular- to fibrous-actin transition. Nature. 457: 441-445.

Osol G, Brekke JF, McElroy-Yaggy K, Gokina NI (2002) Myogenic tone, reactivity, and forced dilatation: a three-phase model of in vitro arterial myogenic behavior. Am J Physiol Heart Circ Physiol 283: H2260-2267.

Paluch E, Heisenberg C-P (2009) Biology and physics of cell shape changes in

development. Curr Biol 19: R790–R799.

Pierre S, Eschenhagen T, Geisslinger G, Scholich K. (2009) Capturing adenylyl cyclases as potential drug targets. Nat Rev Drug Discov. 8: 321-335.

Pinto C, Papa D, Hubner M, Mou TC, Lushington GH, Seifert R. (2008) Activation and inhibition of adenylyl cyclase isoforms by forskolin analogs. J Pharmacol Exp Ther 325: 27-36.

Rappaport R. (1967) Cell division: direct measurement of maximum tension exerted by furrow of echinoderm eggs. Science. 156: 1241-1243.

Riser BL, Cortes P, Zhao X, Bernstein J, Dumler F, Narins RG. (1992) Intraglomerular pressure and mesangial stretching stimulate extracellular matrix formation in the rat. J Clin Invest 90: 1932-1943.

Salisbury JL, Condeelis JS, Satir P. (1980) Role of coated vesicles, microfilaments, and calmodulin in receptor-mediated endocytosis by cultured B lymphoblastoid cells. J Cell Biol 87: 132-141.

Shabb JB. (2001) Physiological substrates of cAMP-dependent protein kinase. Chem. Rev. 101: 2381–2411.

Shih YR, Tseng KF, Lai HY, Lin CH, Lee OK. (2011) Matrix stiffness regulation of integrin-mediated mechanotransduction during osteogenic differentiation of

human mesenchymal stem cells. J Bone Miner Res. 26: 730-738.

Shirazi A, Iizuka K, Fadden P, Mosse C, Somlyo AP, Somlyo AV, Haystead TA. (1994) Purification and characterization of the mammalian myosin light chain phosphatase holoenzyme. The differential effects of the holoenzyme and its subunits on smooth muscle. J Biol Chem 269: 31598-31606.

Somlyo AP, Somlyo AV. (2003) Ca^{2+} sensitivity of smooth muscle and nonmuscle myosin II: modulated by G proteins, kinases, and myosin phosphatase. Physiol Rev. 83: 1325-1358.

Steffen A, Ladwein M, Dimchev GA, Hein A, Schwenkmezger L, Arens S, Ladwein KI, Margit Holleboom J, Schur F, Victor Small J, Schwarz J, Gerhard R, Faix J, Stradal TE, Brakebusch C, Rottner K. (2013) Rac function is crucial for cell migration but is not required for spreading and focal adhesion formation. J Cell Sci 126: 4572-4588.

Sunahara RK, Taussig R. (2002) Isoforms of mammalian adenylyl cyclase: multiplicities of signaling. Mol. Interv. 2: 168–184.

Takizawa N, Koga Y, Ikebe M. (2002) Phosphorylation of CPI17 and myosin binding subunit of type 1 protein phosphatase by p21-activated kinase. Biochem Biophys Res Commun 297: 773-778.

Tamura K, Haga H, Mizutani T, Kawabata K. (2011) Active fluctuation in the cortical cytoskeleton observed by high-speed live-cell scanning probe microscopy. Acta Biomater 7: 3766-3772.

Tesmer JJ, Sprang SR. (1998) The structure, catalytic mechanism and regulation of adenylyl cyclase. Curr. Opin. Struct. Biol. 8:713–719

Tian Y and Laychock SG. (2001) Protein kinase C and calcium regulation of adenylyl cyclase in isolated rat pancreatic islets. Diabetes 50: 2505-2513.

Umemoto S, Bengur AR, Sellers JR. (1989) Effect of multiple phosphorylations of smooth muscle and cytoplasmic myosins on movement in an in vitro motility assay. J Biol Chem. 264: 1431-1436.

Velasco G, Armstrong C, Morrice N, Frame S, Cohen P. (2002) Phosphorylation of the regulatory subunit of smooth muscle protein phosphatase 1M at Thr850 induces its dissociation from myosin. FEBS Lett 527: 101-104.

Vicente-Manzanares M, Koach MA, Whitmore L, Lamers ML, Horwitz AF. (2008) Segregation and activation of myosin IIB creates a rear in migrating cells. J Cell Biol. 183: 543-554.

Vicente-Manzanares M, Ma X, Adelstein RS, Horwitz AR. (2009) Non-muscle myosin II takes centre stage in cell adhesion and migration. Nat Rev Mol Cell

Biol. 10: 778-790.

Weinbaum S, Zhang X, Han Y, Vink H, Cowin SC. (2003) Mechanotransduction and flow across the endothelial glycocalyx. Proc Natl Acad Sci USA. 100: 7988-7995.

Wendt T, Taylor D, Trybus KM, Taylor K. (2001) Three-dimensional image reconstruction of dephosphorylated smooth muscle heavy meromyosin reveals asymmetry in the interaction between myosin heads and placement of subfragment 2. Proc Natl Acad Sci U S A. 98: 4361-4366.

Willoughby D, Cooper DM. (2007) Organization and Ca^{2+} regulation of adenylyl cyclases in cAMP microdomains. Physiol. Rev. 87: 965–1010.

Yanagida T, Arata T, Oosawa F. (1985) Sliding distance of actin filament induced by a myosin crossbridge during one ATP hydrolysis cycle. Nature. 1985 316: 366-369.

Yoshigi M, Hoffman LM, Jensen CC, Yost HJ, Beckerle MC. (2005) Mechanical force mobilizes zyxin from focal adhesions to actin filaments and regulates cytoskel*et al* reinforcement. J Cell Biol 171: 209-215.

Yoshikawa T, Peel SA, Gladstone JR, Davies JE. (1997) Biochemical analysis of the response in rat bone marrow cell cultures to mechanical stimulation. Biomed Mater Eng 7: 369-377.

Acknowledgements

I would like to offer my special thanks to Prof. Hisashi Haga for his constructive comments and suggestion. He has been a tremendous mentor for me. Without his guidance and persistent help this thesis would not have been possible. His advices on both research as well as business manner have been priceless.

I would also like to thank Prof. Kazushige Kawabata and Assistant Prof. Takeomi Mizutani for insightful and incisive comments in discussion. My sincere thanks also goes to Prof. Sasaki, and Prof. Fukui for reviewing this dissertation.

I express cordial gratitude to Misako Imai for her constant encouragements and emotional supports. I also thank other members of the Laboratory of Cell Dynamics for their support in doing the experiments.

I would like to thank my parents Taishi and Hiroko Takemoto for financial support and moral help.